LAWRENCE
LIVERMORE
NATIONAL
LABORATORY

UCRL-JRNL-221379

Insights Into Ground Shock in Jointed Rocks and the Response of Structures There-In

F. E. Heuze, J. P. Morris

May 15, 2006

International Journal of Rock Mechanics and Mining Science

Insights Into Ground Shock in Jointed Rocks and the Response of Structures There-In

F. E. Heuze, J. P. Morris

Abstract

Ground shock in rock masses is created by dynamic events such as rock-bursts, coal bumps or man-made explosions. This article examines two aspects of the phenomenology: the propagation of ground shock and its effects on underground structures. Numerous experiments, at all scales, as well as numerical modeling clearly show that geologic discontinuities have a large influence on ground shock propagation through their actions as wave-guides or as decoupling features. Then, 3-dimensional discrete element (DE) numerical models provide additional insights into the dynamic response of underground structures as influenced by joint orientation, joint spacing, characteristics of the loading pulse (duration, peak velocity, peak displacement), and repeated loadings. It is also shown that in hard rocks the deformability of rock blocks has a negligible influence on tunnel dynamic structural response compared to that of the joint sets or bedding. When viewed together with pictures of underground failures, the 3-D DE models are shown to capture quite well the kinematics of jointed rocks, and their power is illustrated through a very large simulation of an underground facility under dynamic loading.

1. GROUND SHOCK PROPAGATION

1.1 . Introduction

Multiple experiments at various scales have shown the peculiar attributes of ground shock propagation in jointed media. They involved both conventional high explosives and nuclear explosives. They reveal that the presence of geological interfaces such as joints, shears, bedding planes and faults can both guide the ground motions along preferred directions and/or attenuate those motions as they propagate across.

1.2 . Small-scale tests

A classic early result was provided by the ”sugar shot” test [1]. A firecracker was set off in a cardboard box containing an array of sugar cubes, with the results shown in Figure 1. This very inexpensive test ($4.50) showed that damage is propagated farther along directions perpendicular to the two main sets of interfaces. This is because the interfaces are much stiffer in the normal

directions than in shear, and the dynamic motions are more poorly propagated when coming across at less than normal incidence. The result is to shelter part of the domain from maximum damage.

Another example is given by a test on a small cylinder of grout with two parts separated by a slick interface [2]. Velocity gages were placed on either side of the interface. The impulse was created by the detonation of a small charge of PETN explosive (Fig. 2a). The peak velocity was attenuated by a factor of 10 upon crossing the interface between the two pieces (Fig. 2c versus Fig. 2b).

1.3 . Field Tests of ground shock

1.3.1. The Starmet test

Starmet was conducted in 1970 in New Mexico [3, 4]. It involved the detonation of 1980 kg of high explosives in a planar array of 11 vertical holes drilled in granite (Fig. 3a). Near-field motions were recorded by velocity gages and accelerometers grouted in numerous holes. Fig. 3b shows the very large difference in recorded velocity time-histories between two gages located on either side of a shear feature respectively at about 9m and 18m from the explosive source. While the peak velocities are within 25% of each other, the pulse duration has been shortened by a factor of 13, so that the peak displacement is reduced by a factor of about 15 from one side of the shear to the other. This interface has created a large ground motion “decoupling”.

Another component of Starmet was the testing of model missile silos. As shown in Fig. 3c the silos were disabled by shear along joints rather than by crushing.

1.3.2. The Piledriver test

Piledriver was an underground 61-kiloton nuclear test conducted in 1966 in granite at the Nevada Test Site. A particular drift, named DL 0+70, is examined. Its pre-test joint structure was mapped (Fig. 4, after [5]) and its post-test condition was recorded (Fig. 5, after [5]). A 2-dimensional simulation of that drift was performed with the LLNL discrete element DIBS code [6]. The results are shown in Fig. 6. That simple model captures both the roof fall as well as the rubble on the floor. What is particularly interesting, as shown in Fig. 6, is the “gun-barrel” or wave-guide action of two parallel joints on the left side that propel a small number of rock blocks into the opening.

Another example of such wave-guide action of joint sets was demonstrated in a calculation shown in Fig. 7 [6]. A loading pulse of constant magnitude and 2ms duration was applied

perpendicular to the surface of the opening in a dipping joint structure. The velocity vectors at 2msec are still in the original orientation, but after only 10ms they have been reoriented along the principal joint directions.

1.3.3. A high-explosives test in tunnels in Kazakhstan

As part of a joint program between the U. S. government and the Republic of Kazakhstan, a number of tunnels at the former Soviet Union nuclear test site were destroyed. Fig. 8 shows the layout of such a tunnel complex, where a 100-ton high-explosives charge was detonated in the indicated chamber at top right. Geological site characterization revealed the presence of a fault zone intersecting drifts A, B, and D (Fig. 8). The salient feature of that event was that the drift portions on the near–side of the fault from the explosions were destroyed or heavily damaged while those on the other side were undamaged. While some gas-driven fracturing had taken place from the explosive chamber, that dissipated some of the explosion's energy, it is very likely that the fault zone had also sheltered those drifts sections from ground shock.

1.4. Cratering and spalling

1.4.1. The Sulky cratering event

Sulky was a test conducted at the Nevada Test Site in 1964 as part of the Plowshare program, Ninety tons of nuclear explosive were detonated at a depth of 27.4m in dry basalt. Fig. 9 shows three frames from the video of that event. The result was a mound or "retarc" (crater spelled backward…). The peak surface velocity was measured at 26m/s. The early time cavity radius was estimated to be 5m based on calculations with the LLNL SOC hydro-code. A simulation of Sulky was performed with DIBS by putting a forcing function on the surface of that cavity that would result in matching the peak spall velocity [8]. The results of that simulation are shown in Fig. 10. The height and shape of the mound were captured by DIBS. A very interesting feature of Sulky the event was the vertical direction of the ejecta (Fig. 9b). The DIBS simulation reveals the redirection of velocity vectors from a radial to a more vertical direction between 0 and 500ms, while the explosion is creating the shear surfaces forming the initial crater.

1.4.2. Ground surface spall from underground nuclear tests

In several contained nuclear tests in granite in Nevada it was noted that the surface location vertically above the center of the cavity (SGZ, or surface ground zero) rose and then fell back with a return acceleration well in excess of gravity [9, 10]. For example in the Shoal event – 12.5 kilotons at a depth of 340m, in 1963 – the average return acceleration was -1.33g. A generic

simulation was performed with the DIBS code with a cavity at 340m of depth and a forcing function to match the Shoal SGZ peak velocity of 6.5m/s [9]. The layout is shown on Fig. 11a. The DIBS calculation indicated a – 1.46 g return acceleration (Fig. 11b), slightly above the Shoal data. The model captured the phenomenology of the surface layer that stores strain energy upon deforming without breaking and recovers it on the downward motion.

1.5. Summary

This first part of the article was designed to sensitize the reader to several aspects of ground motion propagation in jointed rocks:

- The geological discontinuities (joints, bedding planes, shears, and faults) can act as wave-guides to ground motion, thus accentuating damage or minimizing it in different directions.
- Discontinuities can outright shelter some regions of the rock mass from ground shock damage
- Simulations that discretely include the geological discontinuities can reveal complex aspects of cratering and spall phenomenology. Continuous models would not reveal those aspects.

2. RESPONSE OF STRUCTURES

2.1. Introduction

In this work, the dynamic response of underground facilities in jointed rocks is explored by means of 3-dimensional discrete element modeling performed with the LDEC code [11]. It is appropriate to start with several notes and caveats.

2.1.1. Trade-offs in simulations

When designing analysis models to estimate the "strength" of structures against ground shock competing options will arise in the selection of features for the geology and the structure, as outlined in Table 1.

2.1.2. Type and duration of the simulations

The discrete element calculations typically used 3-D rock islands housing a tunnel or other structure that were loaded on one or more boundaries by velocity pulses. Prior to loading, boundary in-situ stresses were applied and the mesh was allowed to settle for 50ms, followed by the excavation that was allowed to settle for another 50ms. The pulse was then applied and the calculation performed for up to 3000ms to bring everything to rest; see for example Fig. 12, a 13m x 2 x15m island with 3 joint sets of equal 30-cm spacing and 12425 blocks. Non-loaded boundaries were designed as "infinite", so as to eliminate shock reflections.

Table 1. Competing factors affecting the "strength" of facilities under ground shock

Features making the underground facility More resistant to ground shock.	Features making the underground facility less resistant to ground shock
Geology	Geology
Non-continuous joints	Continuous joints
Wider joint spacing	Smaller joint spacing
Dilatant joints	Non-dilatant joints
Higher shear and tensile strength of the joints	Lower shear and tensile strength of the joints
More porous rocks overlying the facility	Less porous rocks overlying the facility
Less water saturation of the voids	More water saturation of the voids
Facility design	Facility design
Smaller span of rock openings	Larger span of rock openings
Rock reinforcement	Un-reinforced rock mass
Tunnel liner	No tunnel lining

2.1.3. Joint set representation in a massively parallel environment

Simulations involving large numbers of rock blocks preferably will be performed in massively parallel environments. That implies that an adequate load balancing is implemented between the multiple processors. Effectively, it means that a fairly even number of blocks will be assigned to each processor and each block would have a reasonably similar number of neighbors. But the real structure of jointed rock masses can be far from fitting these assumptions. As shown in Fig. 13, large blocks will have many neighbors while small blocks have very few. Practically speaking, it is beyond current practice to perform simulations using that kind of block pattern. Typically, joint set spacing in numerical models may range over a factor from say 1 to 5. However, joint intersections may still generate a geologic structure where the volume ratio between biggest and the smallest blocks is quite large.

2.1.4. On the handling of small blocks

In explicit integration scheme, such as employed in LDEC, the time-step is controlled by the smallest block size or minimum distance between interfaces. To prevent extremely small time steps that would greatly prolong the calculations one may merge the smallest blocks with neighbors. However, one should exercise caution when doing so because in real geologies small blocks may fall out in the underground opening and result in instability and possible collapse. That is illustrated in Fig. 14, showing that the selection merge threshold can significantly change the response of the structure. It is advisable to start calculations with the block size distribution resulting from the assigned joint pattern. Any initial instability will indicate that the stand-up time of the structure is very short, if left unsupported

2.1.5. In the matter of persistence of discontinuities

Given the various types of geologic discontinuities, it is clear that their degree of persistence (continuity) can vary. For example, bedding can be quite persistent (Fig. 15) while cross-bedding joints may lack continuity (Fig. 16). Schematics of joint surfaces with various degrees of joint persistence are shown in Fig.17. The influence of joint continuity on tunnel strength will be explored in this work. In LDEC non-persistent joints with a continuity expressed as a percentage are subjected to the drawing of a random number between 0 and 100 each time a joint crosses another set, to determine whether that crossing is allowed.

2.1.6. Use of rigid blocks versus deformable blocks

When modeling hard jointed rock masses there is some merit in making the blocks rigid and the interfaces compliant. The benefit is to speed up the simulations by a significant factor. Typically in this work, calculations with 10000 rigid blocks run to 3000msec on 2 parallel processors with time-steps of the order of a microsecond lasted 30 days. The deformable-block calculations ran about 4 times longer. Using rigid blocks presumes that the rock blocks are not breaking. In fact, this assumption seems to be reasonable, considering some observations made in very high stress environments. Reference [12] indicates that no microscopic damage was identified in the Climax granite subjected to a peak stress of 700MPa in the Piledriver nuclear event. All the tunnel damage was attributed to failure along joints. To examine this question further, twenty-seven calculations were performed on rock islands with variations on two basic geologies containing a tunnel as shown in Fig. 18. The islands are 16m x 1m x 16m, with one block across the thickness. There is a 1MPa confining stress on all boundaries, except the top one that is loaded with a triangular pressure pulse. The tunnel is 4-m wide by 5-m high and the joint spacing is

0.7m. Basic geology 1 has 2 sets dipping at 45 degrees, and basic geology 2 has one set dipping at 20 degrees and the other dipping at 80 degrees. There are respectively 513 and 519 blocks in geologies 1 and 2. The interfaces are compliant and non-dilatant. The normal stiffness is hyperbolic, with an initial slope of 6.0GPa/m increasing to infinity at the maximum joint closure of 1mm; the shear stiffness is 0.3GPa/m, the friction angle is 35^{o}, peak and residual, and the joint tensile strength and cohesion are 0.05MPa. When deformable, the blocks have a Young's modulus of 70GPa and a Poisson's ratio of 0.25. When bolted, the bolting pattern is shown on Fig. 19. The authors are cognizant of the work done in modeling rock bolting of jointed rock over the years ([13] to [17]). In LDEC un-tensioned, grouted rock bolts are implemented using the model described by Lorig [16] that expresses the force exerted by the bolt in terms of the normal and shear deformation of a segment of the bolt in the vicinity of each joint it intersects. Using this approach, the effect of the rock bolts is assumed to be concentrated where the bolt passes through a joint. This assumption is consistent with experimental observations ([13] to [15]).

Comparing the cases with rigid and deformable blocks reveals that only five of them, cases 1-2-22-24-25, show substantial differences (Figs. 20 and 21). In order to obtain insights in as short a time as possible it seems reasonable to start any large series of simulations in hard jointed rocks with models using rigid blocks, and to check on a few random cases whether rock block deformability makes a difference in the final outcome.

All the simulations described in Part 2 of this article were performed with rigid blocks and deformable interfaces.

2.2 Influence of joint set orientation

Two series of analyses were performed to illustrate the influence of joint set orientation on tunnel strength. A selection is results are shown in Figures 22 through 24. Figure 22 compares tunnels in geology 1 under a 3-MPa pulse (Fig. 22a) and geology 2 under a 45-MPa pulse (Fig. 22b). The striking result is that a mere change in joint set orientations, while everything else says equal, has introduced a difference of a factor of more than 15 in tunnel "strength". Another perspective is gained by taking both geologies and changing the dip of one joint set only over a range of values (Figs. 23 and 24). In each case the stability of the opening increases as a joint set dip is flattened, and decreases when it is steepened.

2.3 Influence of joint set spacing

Geologies 1 and 2 are used again to illustrate the influence of joint set spacing on tunnel stability in Figs. 25 and 26. As known to underground practitioners, the stability of openings can be seriously downgraded when the spacing of joint sets decreases. Because of rock block kinematics that degradation may be more severe in some jointing patterns. This is the case in geology 1 as compared to geology 2.

Table 2. Summary of cases analyzed both with rigid and deformable blocks

Case	Geology	Bolts	Peak stress (MPa)	Peak displacement (cm)
1	1	No	0	0
2	1, with joint spacing 35cm	No	0	0
3	1	Yes	0	0
4	1	No	3	1.4
5	1, with 2nd joint set dip 35º	No	3	1.4
6	1, with 2nd joint set dip 25º	No	3	1.4
7	1, with 2nd joint set dip 15º	No	3	1.4
8	1, with 2nd joint set dip 5º	No	3	1.4
9	1	Yes	3	1.4
10	1, with 2nd joint set dip 35º	Yes	3	1.4
11	1	No	6	2.8
12	1	Yes	6	2.8
13	2	No	6	2.8
14	2	No	12	5.6
15	2	No	18	8.4
16	2	No	24	11.2
17	2	No	30	14.0
18	2, with joint spacing 35cm	No	30	14.0
19	2, with 2nd joint set dip 30º	No	30	14.0
20	2, with 2nd joint set dip 40º	No	30	14.0
21	2, with 2nd joint set dip 50º	No	30	14.0
22	2, with 2nd joint set dip 60º	No	30	14.0
23	2, with 2nd joint set dip 30º	Yes	30	14.0
24	2, with 2nd joint set dip 50º	Yes	30	14.0
25	2, with 2nd joint set dip 60º	Yes	30	14.0
26	2	No	36	16.8
27	2	No	45	21.0

2.4 Influence of joint persistence on tunnel stability

Analyses were performed for lined and unlined tunnels in various geologies, labeled 3 to 6. The rock islands with continuous joints are illustrated in Fig. 27, and the specifics of geology and tunnel are summarized in Table 3. Joint persistence of 100% and 50% were compared. Bedding persistence was set at 100%. When lined, the tunnels would have a 1-m thick heavily reinforced concrete liner (1.5% steel area by cross-section) complemented by a 30-cm thick plain concrete floor. Although LDEC can simulate tunnel liners by coupling to DYNA-3D [11], for simplicity this study modeled the liner using LDEC blocks. The reinforced concrete liners in the LDEC simulations were represented with rigid blocks separated by interfaces with a cohesion and tensile strength corresponding to the rebar crossing through those interface. That value was 4.2MPa for a 1-m thick liner. Clearly, this is a coarse approximation but it is thought to be useful in trying to capture the role played by the liner under dynamic loading.

Table 3. Rock island geology and tunnel metrics for examination of the effect of joint persistence on tunnel stability (DD= dip azimuth; DA=dip angle; W=tunnel width; H=tunnel height)

Geology	Bedding and joint sets	Spacing	Tunnel	Rock island
3	Bedding : DD, 45 ; DA, 80 Joint set 1: DD, 135 ; DA 90 Joint set 2: DD, 225 ; DD 10	12cm 50cm 50cm	W = 3.0m H = 3.2m	10m x 3m x10m
4	Bedding : DD, 360 ; DA, 0 Joint set 1: DD, 0 ; DA, 90 Joint set 2: DD, 90 ; DA, 90	30cm 60cm 60cm	W = 6.0m H = 3.7m	20m x 3m x18m
5	Bedding : DD, 180 ; DA, 25 Joint set 1: DD, 22.5 ; DA, 90 Joint set 2: DD, 45 ; DA, 90 Joint set 3: DD, 67.5 ; DA, 90 Joint set 4: DD, 315 ; DA, 90 Joint set 5: DD, 337.5; DA, 90	60cm 60cm 60cm 60cm 60cm 60cm	W = 6.0m H = 4.5m	18m x 2m x 17m
6	Joint set 1: DD, 240 ; DA, 40 Joint set 2: DD, 60 ; DA, 40 Joint set 3: DD, 150 ; DA, 60	30cm 30cm 30cm	W = 4.3m H = 4.5m	13m x 2m x 154m

2.4.1. Unlined tunnels

The triangular velocity pulses applied to the top boundary of each rock island with unlined tunnels are summarized in Table 4. The tunnel in geology 3 was rock bolted (Fig. 28), and those in geologies 4-6 were not.

Figs. 29 through 32 show the results of the simulations. A conspicuous and expected consequence of decreasing joint set persistence is to decrease the number of blocks in a rock island of a given size.

Table 4. Velocity pulses applied to the top of rock islands in geologies 3 to 6 – unlined tunnels

Geology	Rise time (ms)	Peak velocity (m/s)	Duration (ms)	Peak displacement (cm)
3	5	40	20	40
4	5	20	25	25
5	10	20	40	40
6	10	60	15	45

One could infer that this reduction, which automatically increases the mean size of rock blocks, would automatically result in an increase in tunnel stability. This is the case in all but one of the four cases analyzed. That exception demonstrates that it is not only block size but also the kinematic interaction between blocks that eventually may destabilize a tunnel. In other words, a single key block moving out may initiate a collapse.

2.4.2. Lined tunnels

Lined tunnels were set in geologies 4 to 6. The openings have the same size as those of the unlined tunnels discussed above. The velocity pulses are summarized in Table 5. Tunnels in geologies 4 and 5 were loaded with a vertical velocity pulse on the top boundary, as was the case for unlined tunnels, and the tunnel in geology 6 was loaded with the same pulse normal to both the top and right boundaries.

Table 5. Velocity pulses applied to rock islands with lined tunnels in geologies 4 to 6

Geology	Rise time (ms)	Peak velocity (m/s)	Duration (ms)	Peak displacement (cm)
4 top	10	30	60	90
5 top	2	40	30	60
6 top, and right	10	12	50	30

Figs. 33 through 35 show the results of the simulations. As previously noted, the non-continuous joint set calculations have markedly fewer blocks. The ground shock effects are somewhat mixed. It appears that the liner arch is consistently more damaged when joints are continuous, but that the floor damage seems to be higher with non-persistent joints.

2.5. Influence of loading pulse characteristics on tunnel stability

The rock island with tunnel in geology 1 (Fig. 27a) was used to examine the effect of the velocity pulse characteristics on tunnel stability. It was presumed at the outset that the amount of damage could be related to the total displacement created by the pulse, compared to the minimum spacing of the joint sets. Then two series of calculations were performed, one with a constant velocity pulse and changing duration that would vary the total displacement, and the other with a constant displacement created by increasing the peak velocity and decreasing the pulse duration. Fig. 36 shows the effect of a 5m/s peak velocity pulse of various durations creating total displacements from 3.125 to 50cm. While it is clear that the tunnel damage increases from increasing pulse duration that increase can hardly be quantitatively related to total displacement.

Fig. 37 shows the effect of a 12.5cm total displacement pulse with peak velocities increasing from 1m/s to 20m/s. While the damage increases with peak velocity it is again difficult to quantitatively relate it to the peak velocity.

Although these simulations are a very small subset of conceivable possibilities regarding geologies, tunnels, and pulses, it appears that one will need to study the specifics of each loading pulse to ascertain its effects on a given tunnel.

2.6. Effects of repeated loadings on tunnel stability

It could be assumed that tunnels under repeated loadings would sustain cumulative damages that would decrease their stability more and more with each ground shock. In order to gain insights into that question several simulations were performed for both unlined and lined tunnels under a variety of successive impacts.

2.6.1. Successive loadings on unlined tunnels

The first example is using the rock island and tunnel of geology 3 (Fig. 27a). Three successive pulses were applied normal to the top boundary of the rock island. The pulses and their effects are illustrated in Fig. 38. The very noticeable result is that the first ground shock created an arch stable enough that it resisted two additional loadings, each being stronger than the preceding one.

Examples of such arch geometry can be found at sites exposed to severe ground shock such as shown in Fig. 39, although none has been documented to resist subsequent stronger shocks.

The second example uses the rock island and tunnel of geology 4 (Fig. 27b). It that case, the same pulse (Fig. 40a) was applied twice in sequence normal to the top of the rock island. The effects are shown in Figs. 40b and 40c. Unlike in the previous example, the first application of ground shock creates some partial but not critical damage whereas the repeat application destroys the tunnel.

2.6.2. Successive loadings on a lined tunnel

Rock island and geology 5 are as shown in Fig. 27c, and the tunnel has a 1-m thick reinforced concrete liner and no invert lining. The pulse twice as strong as earlier is applied twice again. Pulse and effects are shown in Fig. 41. After the liner sustained the first ground shock with little damage the second loading had no further effect.

2.7. Some reality checks

While numerical models have given impressive insights in the behavior of jointed rock masses it is wise to try and compare their results to known phenomenology. Fig. 42 to 44 present several such comparisons. Note that the LDEC frames are not related to any simulation of the events in the photographs. In Fig. 42 the steel support has frozen in time and space the buckling of thin coal-measure rock layers due to a coal bump. LDEC is showing such a behavior in a calculation involving geology 1 with 35-cm joint spacing. That conspicuous buckling did not occur in geology 1 when the joint spacing was 70cm. In Figs. 43 and 44 the shape of the roof arch created by a rock burst changes with the joint pattern. Calculations performed with rock islands in geologies 1 and 2 showed examples of such changes.

2.8. The dawn of a new area in large-scale 3-D simulations of facilities in jointed rocks

Access to a new massively parallel computer system at the authors' institution enabled a simulation of greater size and complexity than had previously been possible. The underground complex shown in Fig. 45, without its accesses to the surface, spans 60m in each direction and includes chambers on two levels, a couple of smaller drifts, and a shaft. The lower level has three sections labeled L1, L2, and L3. The height and width of the openings are: upper chamber 7mx7m, upper small drift 2mx2m, and lower drift sections 5mx5m. The three joint sets are:

- Set 1: dip direction 0^{o}, dip angle 10^{o}, continuous
- Set 2: dip direction 180^{o}, dip angle 75^{o}, can be non-persistent

- Set 3: dip direction 90 ^{o}, dip angle 90 ^{o}, can be non-persistent

The model has 8 million blocks and 100 million contact elements. The blocks are rigid and the interfaces are compliant. The horizontal top of the rock island containing the tunnel complex is 25m above the crown of the upper chamber. It was subjected to a vertical triangular velocity pulse that resulted in a peak velocity of 4m/s at the roof of the upper chamber with a rise time of 1ms and a decay time of 19ms. So, the peak displacement was 4cm. Calculations performed on 3840 parallel processors ran to 600ms of real time in 4 days (42 years of CPU). Two geological models were considered in this study, one with continuous joints and the other with non-persistent (i.e., randomized) joints. Figure 46 shows an example of the randomized jointing present in the non-persistent model geology. The block boundaries not aligned with joint sets are created by further subdivisions of blocks above a certain size or aspect ratio. In both geologies discussed here, the joint patterns resulted in typical block sizes of 30 cm The effect of the loading pulse in the geology with non-persistent joints is illustrated in Figs. 47 to 50. On the upper level, it is interesting to note that while the upper large chamber is completely destroyed, the small adjacent drift experiences a range of response going from full collapse close to the large opening, where the intersection degrades tunnel strength, to no damage at some distance. On the lower level one notes that the intersection of the shaft and L3 is collapsed while the nearby intersection of L2 and L3 is stable. Fig. 51 compares the velocity fields of the two simulations, with and without persistent joints, at 30ms in a cross-section through the upper chamber and the upper small drift. Results differ in several ways:

- Persistent joint sets tend to channel the ground shock, resulting in variations in wave speed with the direction of propagation. They also allow shear motion along the entire length of the sets, resulting in large “chimneying” above collapsed tunnels sections
- Non-persistent joints create more diffraction around underground openings. They also distribute the ground shock more uniformly. So, some locations will have stronger and others will have weaker ground shock intensity than with continuous joints.

Summary

Experiments at multiple scales and numerical modeling performed over several decades have combined to give revealing insights into the effects of strong ground motions in jointed rock masses. Summary and conclusions from this article are grouped under three headings.

Ground shock

Jointed rocks act as wave-guides in propagating ground shocks. The interfaces being much stiffer normally across than in a parallel direction will focus the waves in directions normal to the interfaces thus sheltering some regions of the rock mass from the most severe effects.

Significant geologic discontinuities such as faults and shears can decouple the ground shock from one side to the other, particularly when the shock is coming tangentially to the discontinuity. This provides dramatic reductions in the effects of the shock waves.

Numerical modeling

Calculations must be pursued to a long enough real time that the rock mass has reached an equilibrium. This could mean thousands of milliseconds.

Modeling of jointed rocks must include discrete blocks and the interfaces with adjacent blocks. It also must be 3-dimensional. Practically speaking, that puts 3-D discrete element models in a leading position to provide realistic simulations and it implies that these large calculations preferably should be performed in massively parallel environments.

Even though these environments are available, it is possible that the rock block population cannot be distributed in a regular enough fashion among multiple processors thus making it impossible to perform large simulations. The only practical solution may be to employ a less complex representation of the rock mass so that it can be subdivided into domains with somewhat similar numbers of blocks.

Multiple calculations done both with rigid blocks and deformable blocks indicate that the discontinuities control the kinematics of hard jointed rock masses and that most rigid block simulations with compliant interfaces will do an appropriate job of modeling. In turn, that will shorten the length of the simulations by an appreciable factor.

Another way to keep simulations within shorter length is to merge the smallest blocks with larger adjacent blocks so as to increase the minimum time-step in explicit calculations. However, this may introduce a stability of the structures that would not exist were the smallest blocks kept in play. Alternatively, deleting the smallest blocks may provide a lower-bound estimate of the stability of the structure.

Some discontinuities such as bedding tend to be rather persistent, but joint sets often are not. Even though it is difficult to quantify it in the field, the degree of continuity should be a parameter of calculations involving structures in rock since it can have a large influence on response to ground shock.

Response of underground structures

Observations under ground shock of several 100 MPa's have shown that movements along discontinuities rather than rock stress control the failure of tunnels in jointed rocks.

The orientation of joint sets can results in dramatic differences in the rock structures to ground shock. A simple example was given where the difference was a factor of 15.

As is well known to underground practitioners, a decrease in the spacing of joints can also create substantial weakening of a rock structure. That phenomenology was illustrated in this article.

It could be postulated that the severity of ground shock effects on structures could be related to the amount of permanent displacement compared to the minimum joint spacing. That assumption was not validated in an extensive series of calculations. It is conclude that both the peak strength (such as peak velocity) and the duration of ground shock must be investigated to obtain realistic estimates of effects.

A common assumption that repeated loadings will create cumulative damage was not substantiated in all cases. Some combinations of geology and structure characteristics will results in a stable shape of un-reinforced openings after the first shock. For lined subsequent similar loadings will not create more distress.

The influence of the continuity (or persistence) of joint sets is noticeable in several ways:

- Persistent joint sets tend to channel the ground shock, resulting in variations in wave speed with the direction of propagation. They also allow shear motion along the entire length of the sets, resulting in large "chimneying" above collapsed tunnels sections

- Non-persistent joints create more diffraction around underground openings. They also distribute the ground shock more uniformly. So, some locations will have stronger and others will have weaker ground shock intensity than with continuous joints.

Acknowledgments

This work was performed under the auspices of the U. S. DOE by U.C. LLNL under contract W-7405-Eng-48. The authors are grateful to several former and present LLNL colleagues who, over the past twenty years, have contributed to parts of the work described in this article: M. Bonner, T. Butkovich, D. Maddix, W. Moran, M. Rubin, R. Shaffer, and O. Walton.

References

[1] Melzer, S. The "Sugar Shot" test series. Unnumbered U. S. Air Force Weapons Laboratory Report, Albuquerque, New Mexico, 1970, 6p.

[2] Fogel, M. B., Kilb, D. L., Nagy, G., Florence, A. L. Experimental and calculational study of wave-fault interaction. Proc. 4th symposium on containment of underground nuclear explosions, Colorado Springs, CO, 1987, pp 81-89 (NTIS, Springfield, VA).

[3] Blouin, S. E., Kaiser, J. V. Jr., Project Starmet. Volume1: Ground motion data, Air Force Weapons Laboratory, Albuquerque, New Mexico, Report AFWL-TR-72-68, 1972 (NTIS, Springfield, VA).

[4] Blouin, S. Block motion from detonation of near-surface explosive arrays, U. S. Army Cold Regions Research and Engineering Laboratory, Hanover, New Hampshire. Report CRREL 80-26, 1980 (NTIS, Springfield, VA).

[5] Goodman, R. E. Effects of joints on the strength of tunnels. University of California, Berkeley technical report no. 5 to the U. S. Army Corps of Engineers, Omaha, Nebraska. September, 1968, 200p. (NTIS, Springfield, VA).

[6] Walton, O. R., Maddix, D. M., Butkovich, T. R., Heuze, F. E. Redirection of dynamic compressive waves in materials with nearly orthogonal and random joint sets. ASME v.117, Recent advances in mechanics of structured continua, 1991, pp. 65-72. (ASME, New York).

[7] Anonymous, Tunnel 214 post-experiment survey report, report from the National Nuclear Center of Kazakhstan under U.S. contract DSWA01-98-C-0016-P00006 (Item 0070), 1999.

[8] Heuze, F. E., Walton, O. R., Maddix, D. M., Shaffer, R. J., Butkovich, T. R. Analysis of explosions in hard rock: the power of discrete element modeling, Comprehensive Rock Engineering, v. 2, pp. 387-413, 1993 (Pergamon Press, Oxford, U.K.).

[9] Hoffman, V. and Sauer, F., Operation Flint Lock, shot Pile Driver, project officers report - project 1.1, POR-4000, 139pp., June 3, 1969.

[10] Weart, W., Project Shoal, Free-field earth motions, and spalling measurements in granite, VUF-2001, 99pp., February 1965.

[11] Morris, J. P., Rubin, M. B., Blair, S. C., Glenn, L. A., and Heuze, F. E., Simulations of underground structures subjected to dynamic loading, using the Distinct Element method", Engineering Computations, v. 21, n. 2/3/4, pp. 384-408, 2004.

[12] Godfrey, C. "Dynamic Strength of In-Situ Rock", Proc. 3rd Congress ISRM, Denver, CO, v. II-A, pp. 398-403, 1974 (U. S. National Academy of Sciences, Washington, D.C.).

[13] Heuze, F. E. and Goodman, R. E., Finite element and physical model studies of tunnel reinforcement in rock, Proc. 15th U.S. Symposium on Rock Mechanics, Rapid City, S. D., September, pp 37-67, (ASCE, New York), 1973.

[14] Bjurstrom, S., Shear strength of hard rock joints reinforced by grouted un-tensioned bolts, Proc. 3rd Congress ISRM, Denver, CO, v. II-B, pp. 1194-1199, 1974 (U. S. National Academy of Sciences, Washington, D.C.).

[15] Pells, P. J. N., The behaviour of fully bonded rock bolts, Proc. 3rd Congress ISRM, Denver, CO, v. II-B, pp. 1212-1217, 1974 (U. S. National Academy of Sciences, Washington, D.C.).

[16] Lorig, L. G., A simple numerical representation of fully bonded passive rock reinforcement for hard rocks, Computers and Geotechnics, v. 1, 1985, pp.79-97

[17] Grasselli, G., "3-D behavior of bolted rock joints: experimental and numerical study", Int. J. of Rock Mechanics and Mining Sciences, v. 42, n. 1, 2005, pp. 13-24.

[18] Hatzor, Y. H., and Feintuch, A. "The Joint Intersection Probability", Int. J. of Rock Mechanics and Mining Sciences, v. 42, 2005, pp. 531-541.

[19] Pariseau, W. G. "Threshold Phenomena and Equivalent Strength Associated with Joint Persistence", Proc. 40th U.S. Rock Mechanics Symposium, Anchorage, AK, paper 686, 2005 (ARMA, Alexandria, VA).

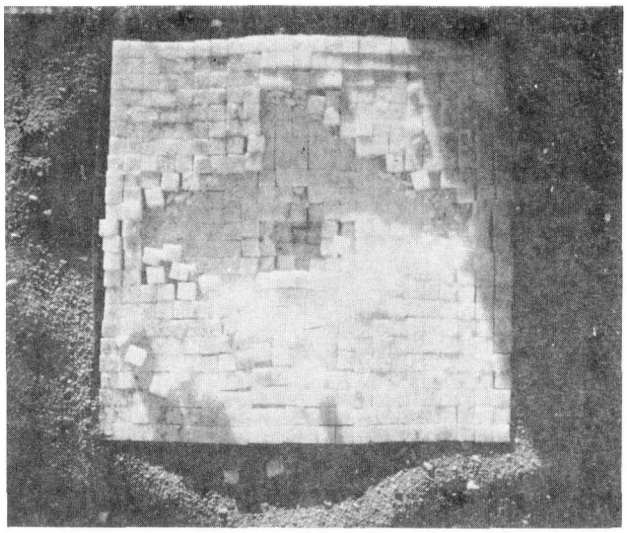

Figure 1. Result of the ”sugar shot” experiment [1]

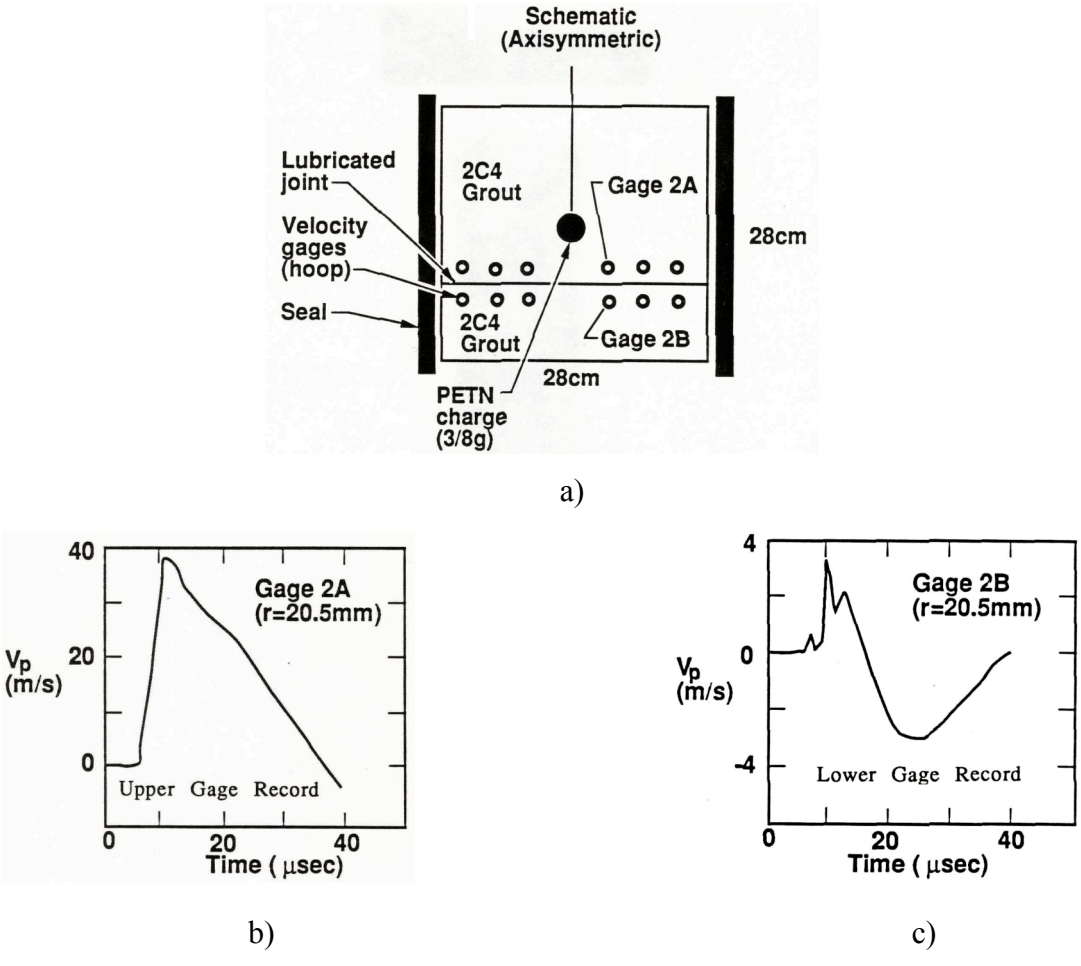

Figure 2. Propagation of shock wave across a slick interface [2]

a) Lay-out of the test bed

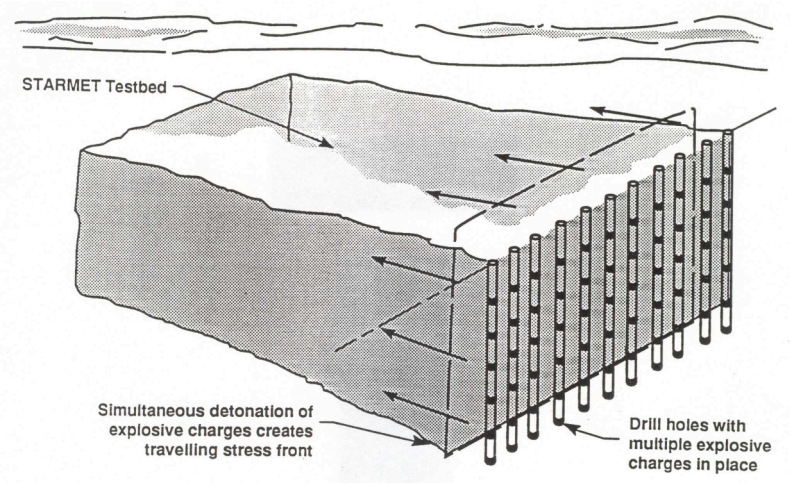

b) Comparison of velocity records

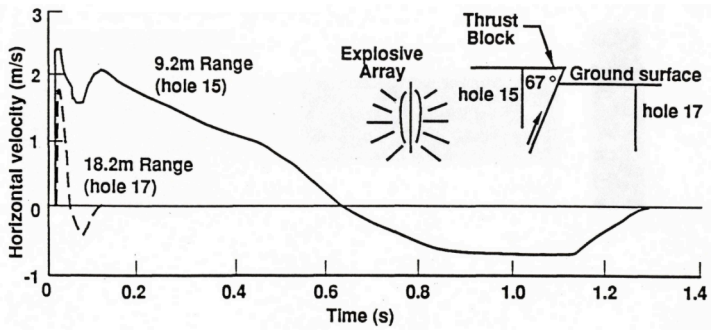

c) effects on model silos

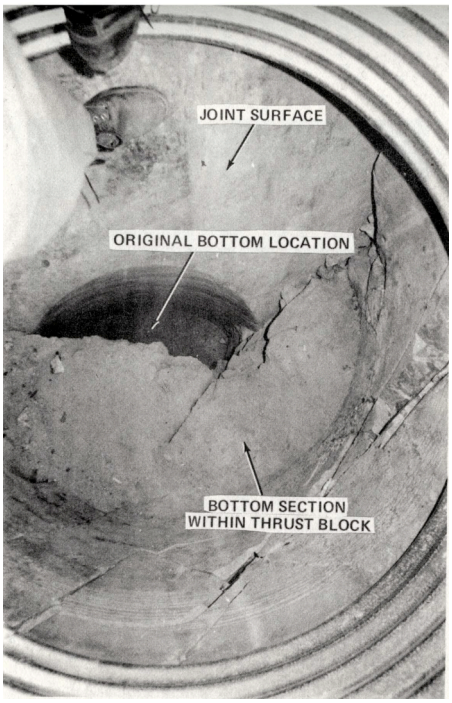

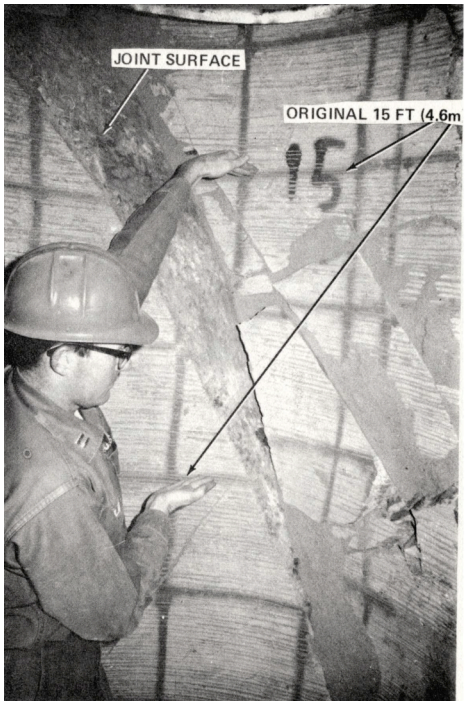

Figure 3. Results of the Starmet HE test [3, 4]

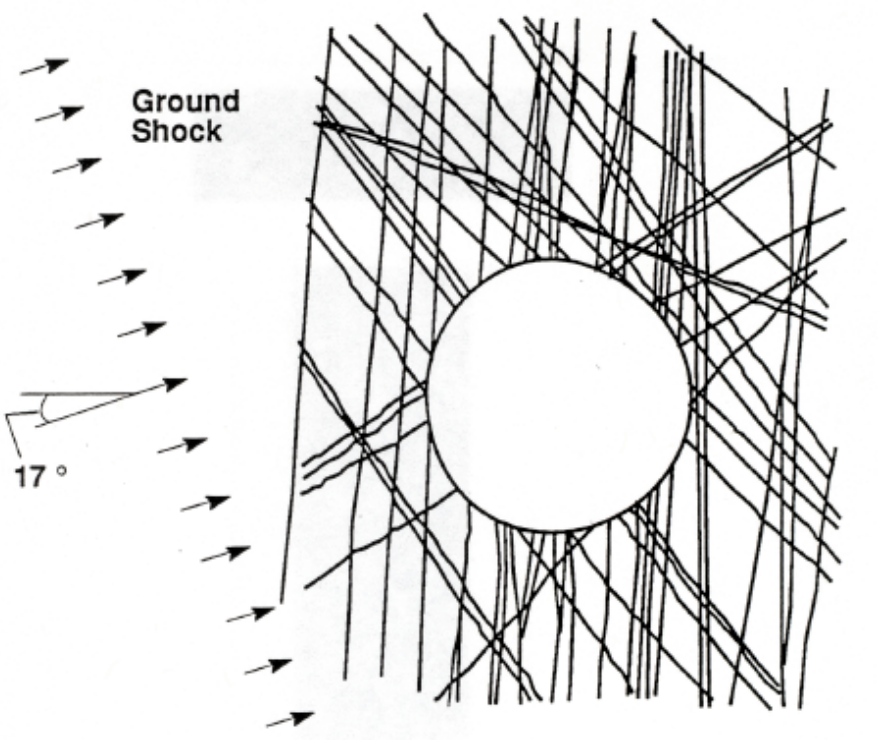

Fig. 4. Pre-test joint mapping of Piledriver drift DL0+70 [5]

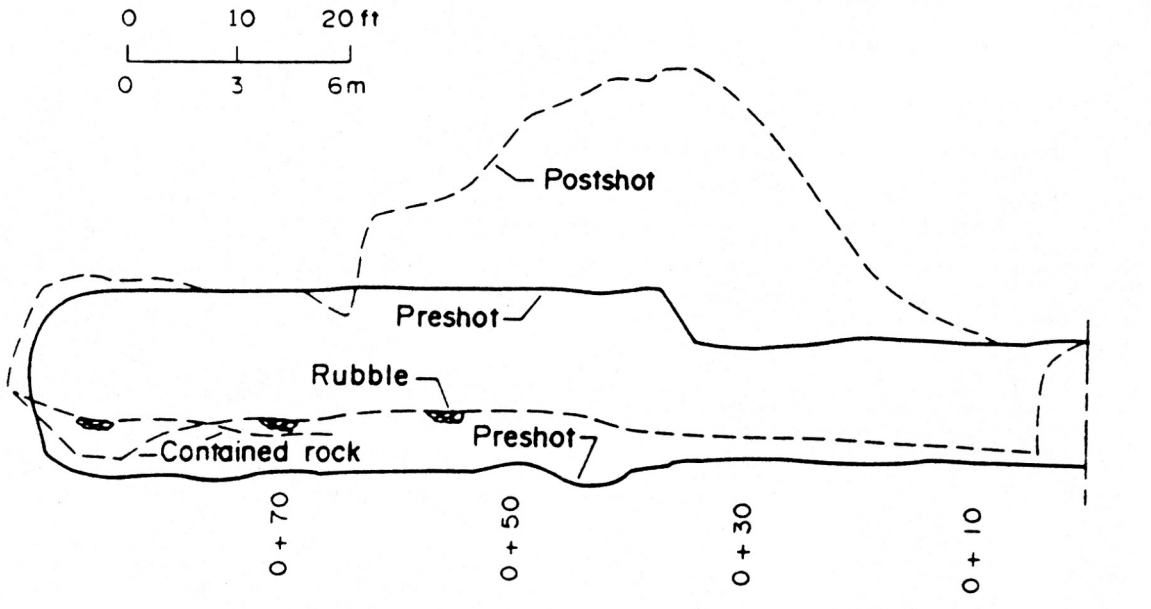

Figure 5. Post-test condition of Piledriver drift DL0+70 [5]

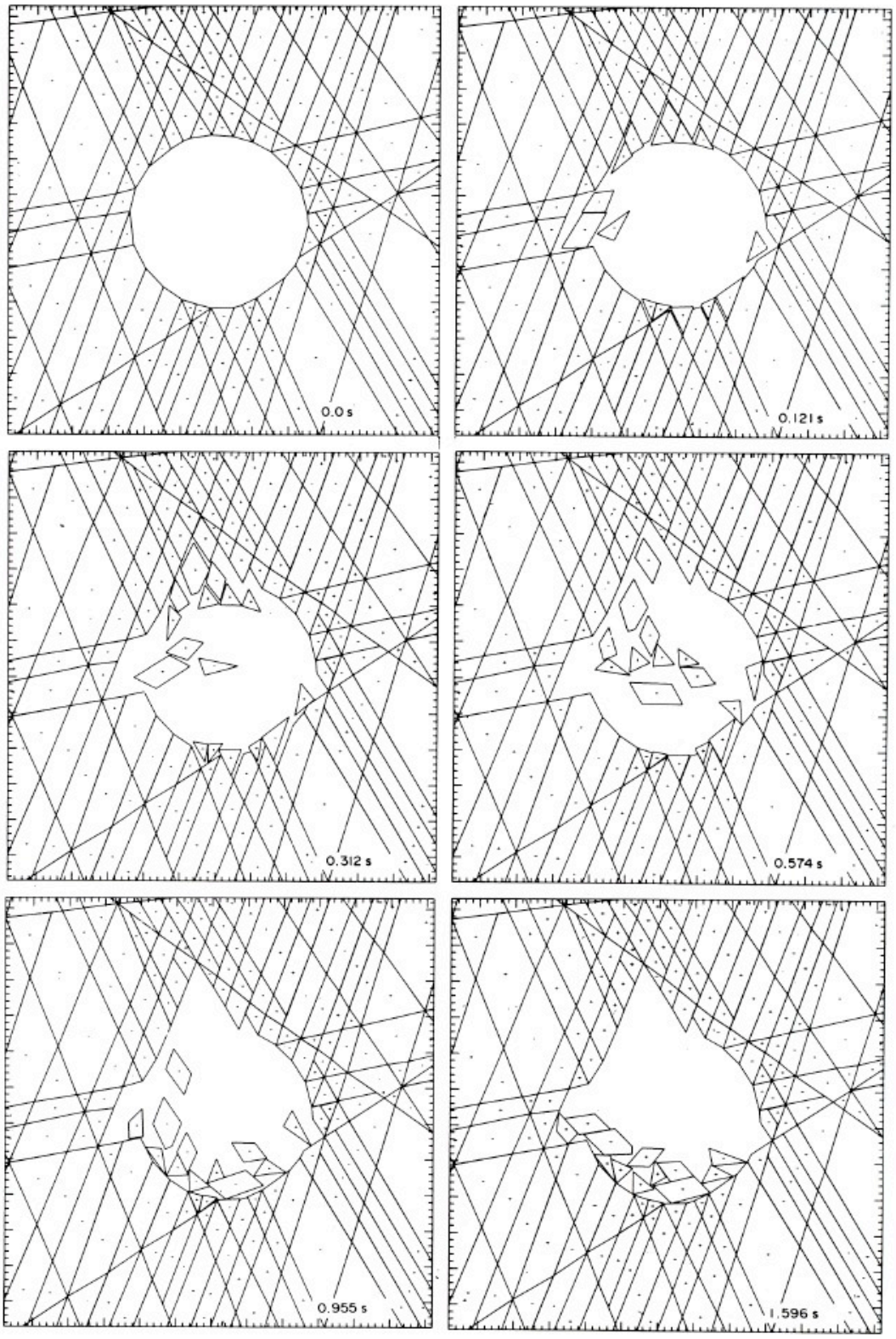

Fig. 6. DIBS discrete element simulation of Piledriver drift DL0+70 under ground shock, showing the wave-guide action of parallel joints on the left-hand side.

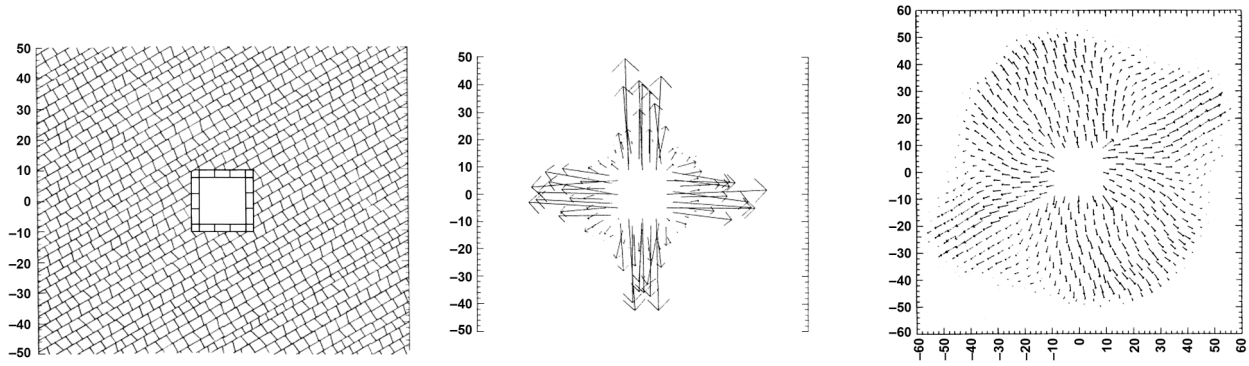

a) initial condition b) velocity vectors at 2ms c) velocity vectors at 10ms

Fig. 7. Wave-guide action of joint sets redirecting ground shock along principal structural directions [6]

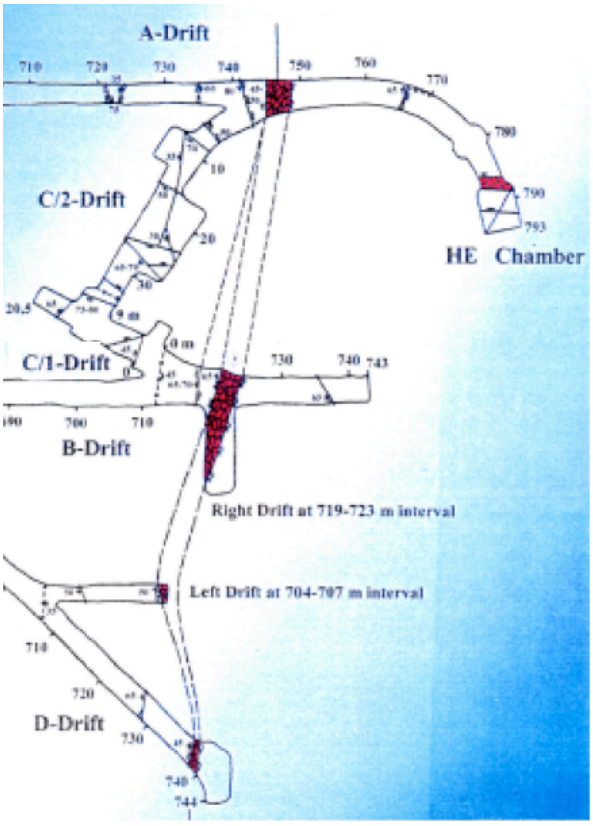

Fig. 8. Layout of a HE test in a tunnel complex in Kazakhstan [7]

Fig. 9. Snapshots from the 90-ton Sulky nuclear cratering event in Nevada

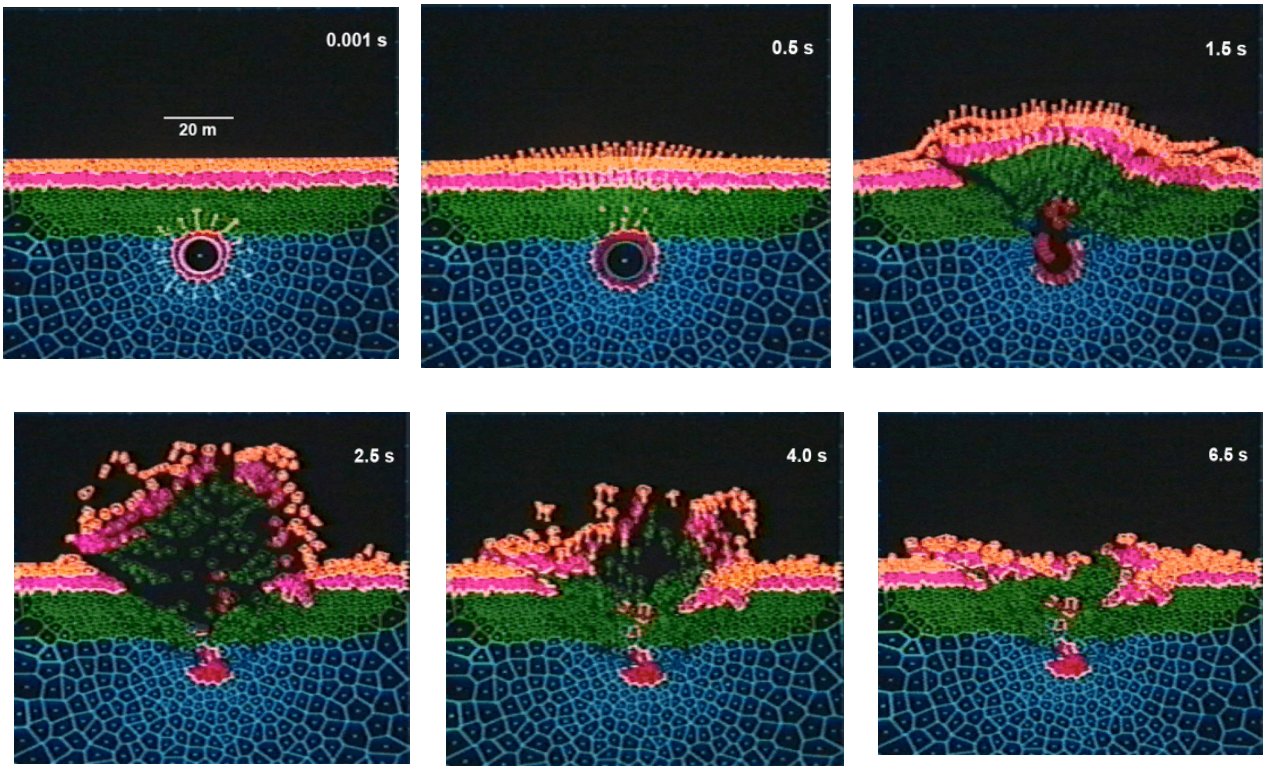

Fig. 10. Time-sequence of the DIBS discrete element simulation of the Sulky event [8]

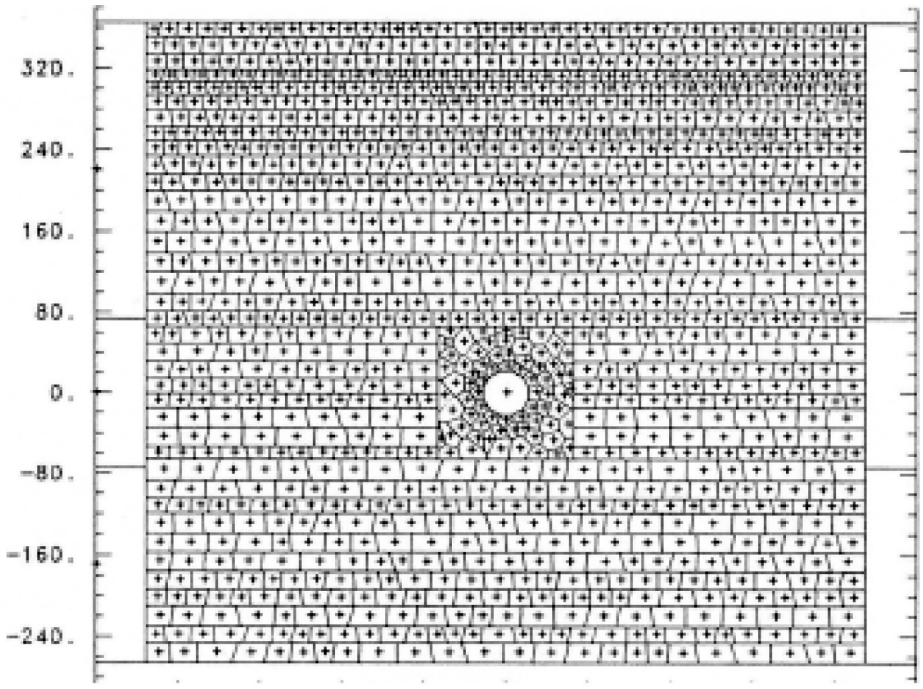

a) Layout of the DIBS Shoal-like generic model

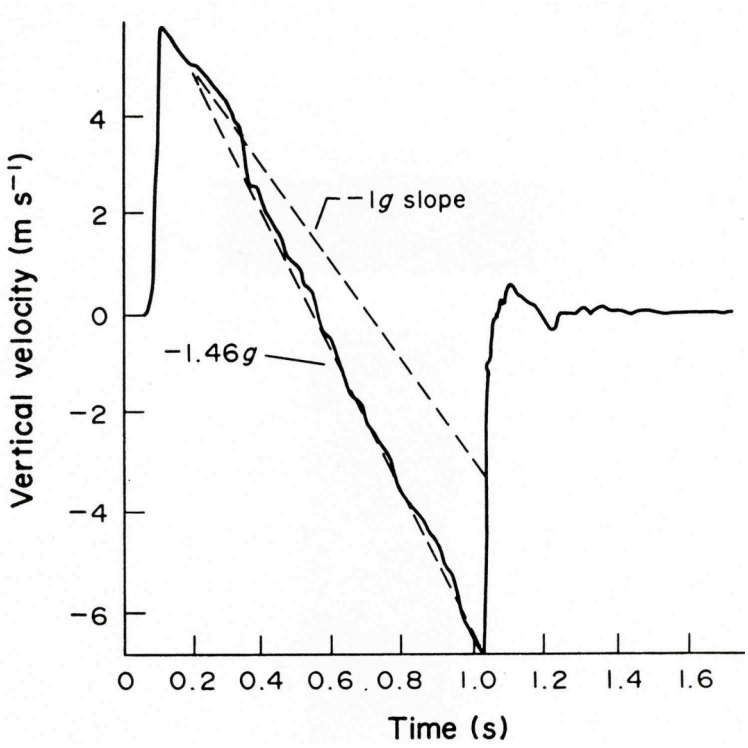

b) Calculated velocity time-history of SGZ

Fig.11. DIBS simulation of a Shoal-like contained underground nuclear test [8]

a) Rock island, with 3 joint sets and 12425 blocks, loaded on the top with a velocity pulse

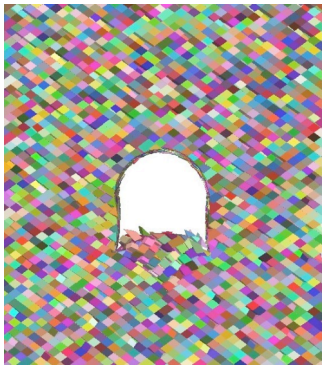

b) 500ms

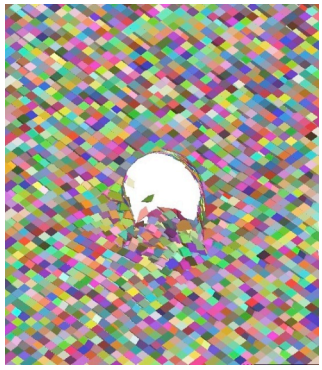

c) 1000ms

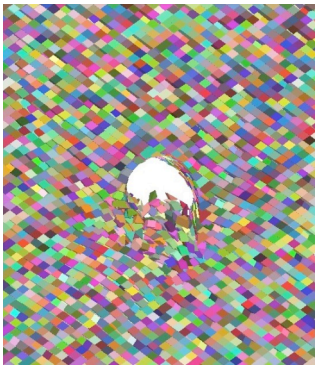

d) 1500ms

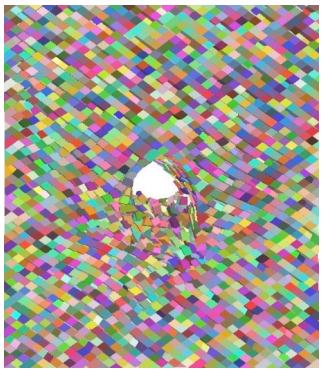

e) 2000ms

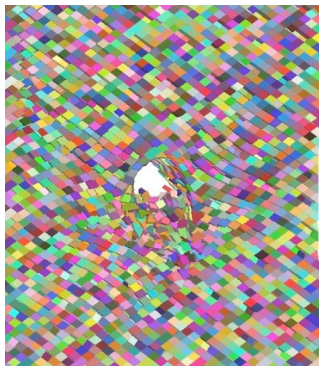

f) 2500ms

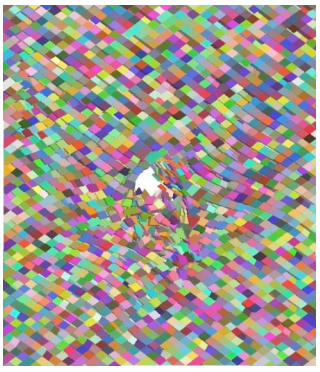

g) 3000ms

Fig. 12. Time-sequence of failure for the tunnel in the rock island

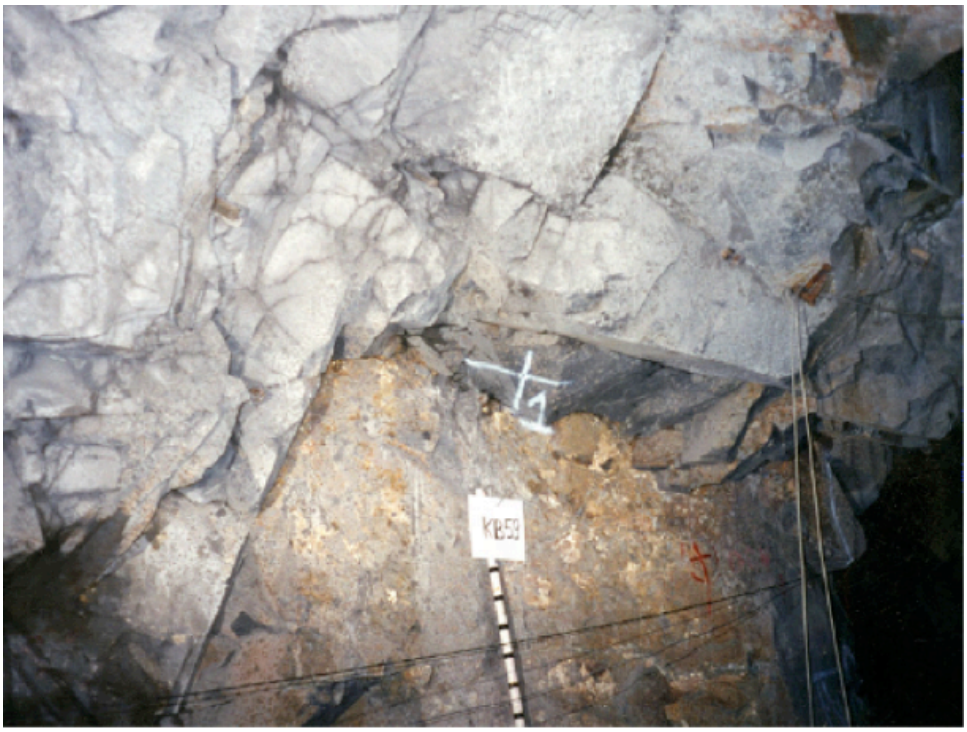

Fig.13. Close-up of the wall surface of a tunnel in hard rock, after [7], showing big differences in the size of contiguous rock blocks

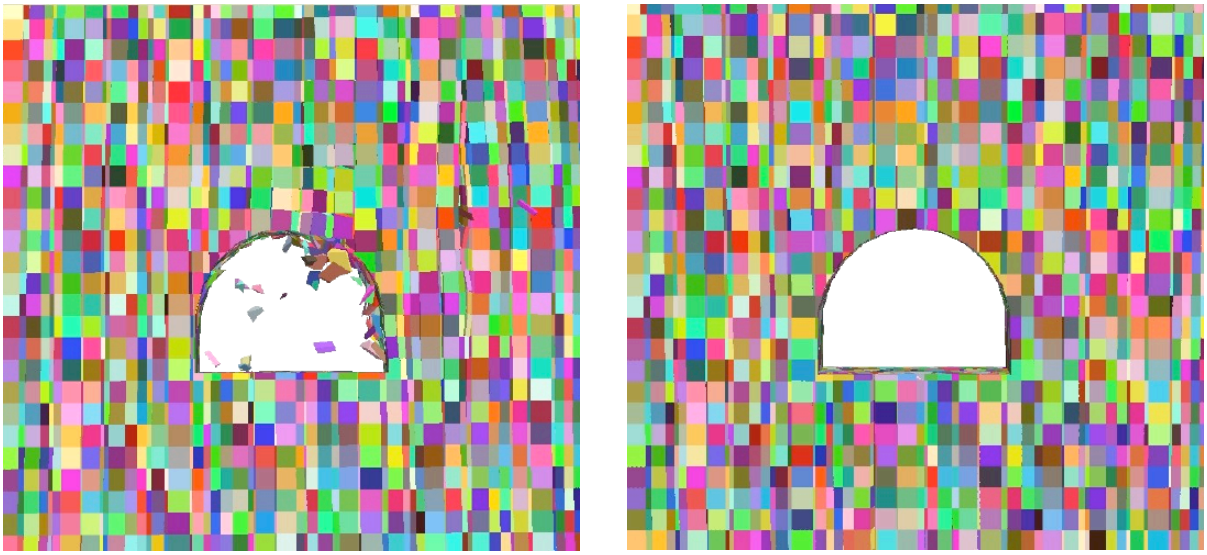

a) Minimum block mass set at 10kg

b) Minimum block mass set at 25kg

Fig. 14. Influence of the block-merging threshold on tunnel behavior; gravity loading example.

Fig. 15. “Goosenecks” of the San Juan river, Utah, showing extensive persistence of the bedding (Air photo by F. Heuze)

Fig. 16. Lack of continuity of cross-bedding joints in a gypsum quarry, after [18]

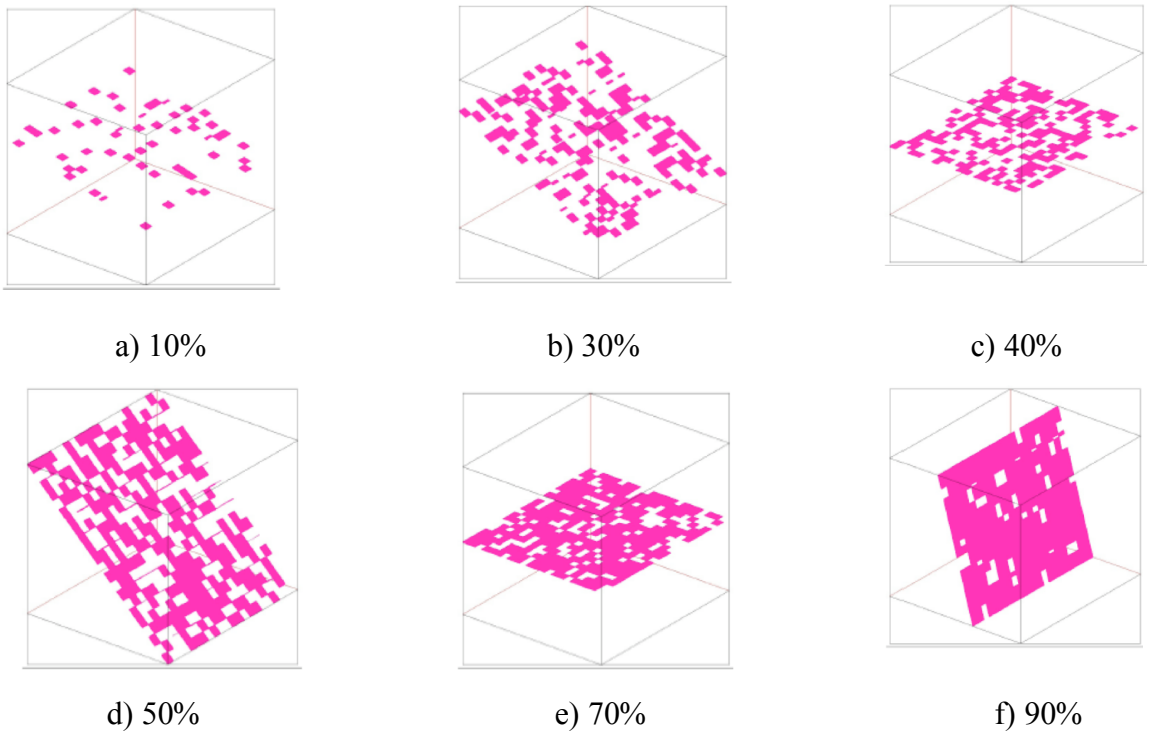

a) 10% b) 30% c) 40%

d) 50% e) 70% f) 90%

Fig. 17. Schematics of joint planes with various degrees of joint continuity; colored areas are joint planes and white areas are rock bridges, after [19]

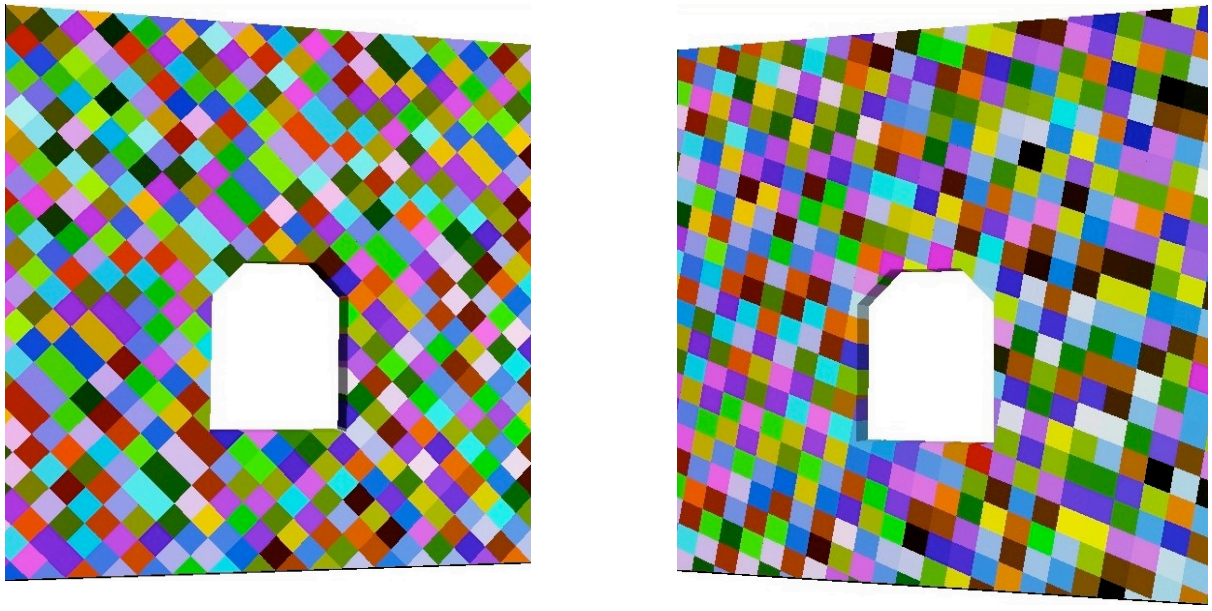

Geology 1 Geology 2

Fig. 18. Rock islands with tunnel in geologies 1 and 2

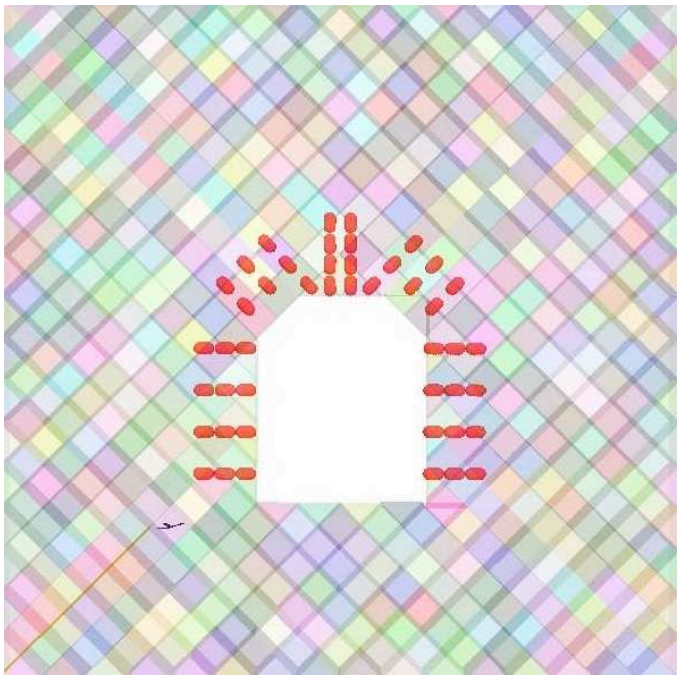

Fig. 19. Bolting pattern when used for tunnels in geologies 1 and 2

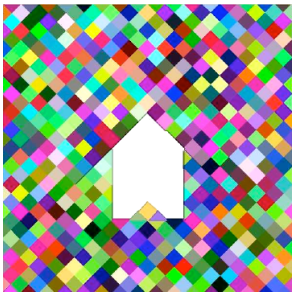

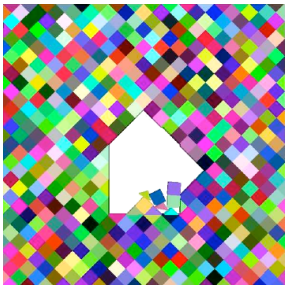

Case 1

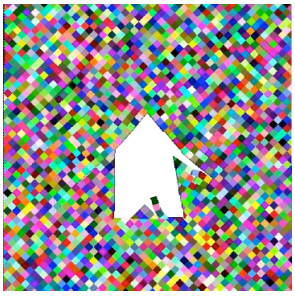

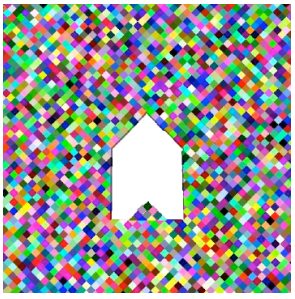

Case 2

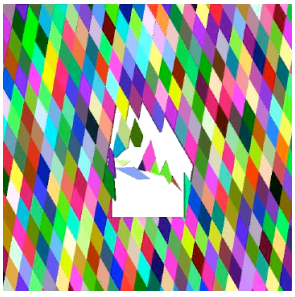

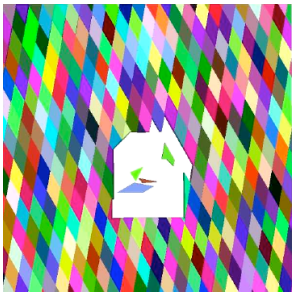

Case 22

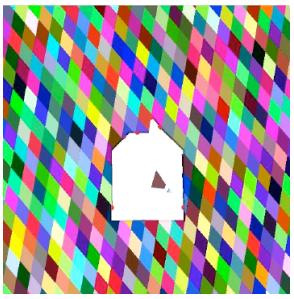

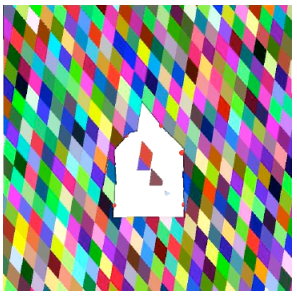

Case 24

Case 25

Fig. 20 Simulations with rigid blocks

Fig. 21 Simulations with deformable blocks

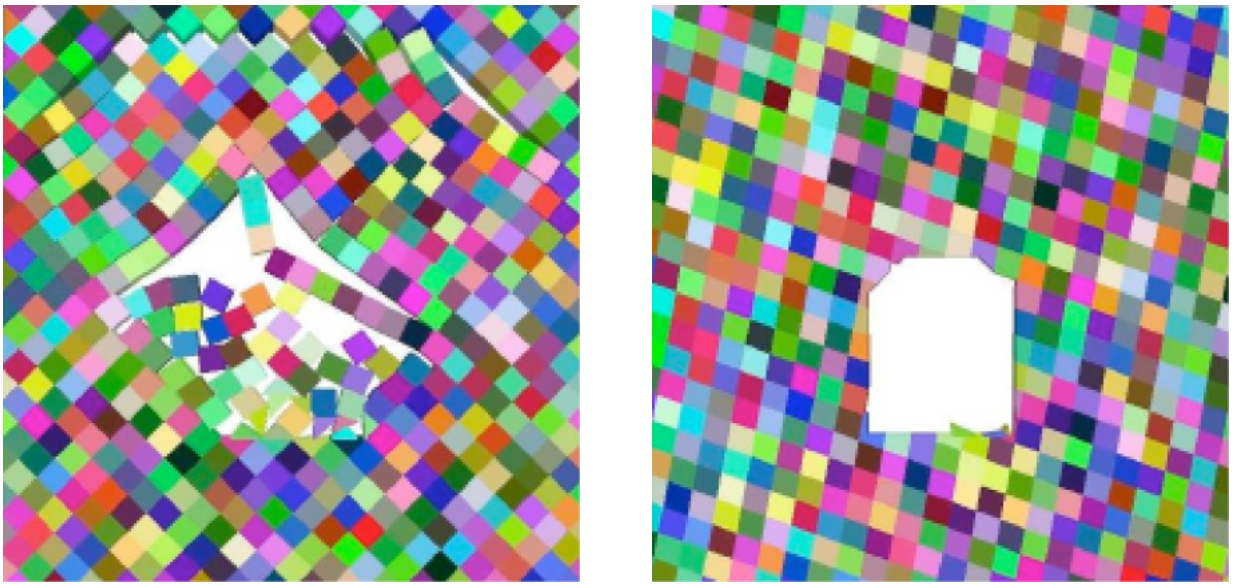

a) Tunnel in geology 1 under a 3MPA pulse b) Tunnel in geology 2 under a 45-MPa pulse

Fig. 22. Comparison of strength for two un-reinforced tunnels in different jointing patterns

a) Joint set 2 dipping 45 degrees

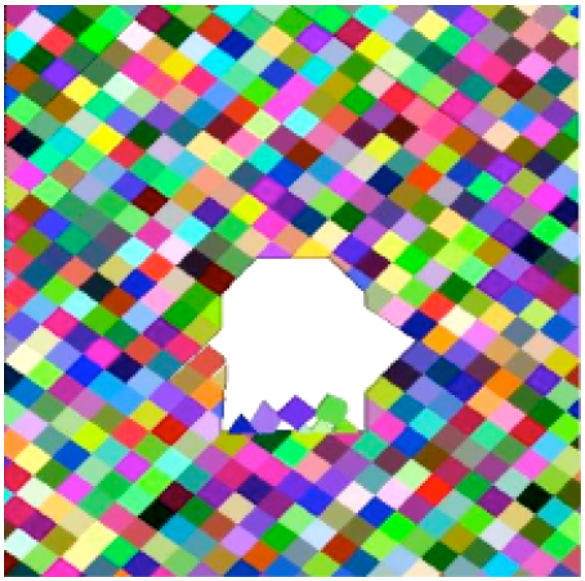

b) Joint set 2 dipping 35 degrees

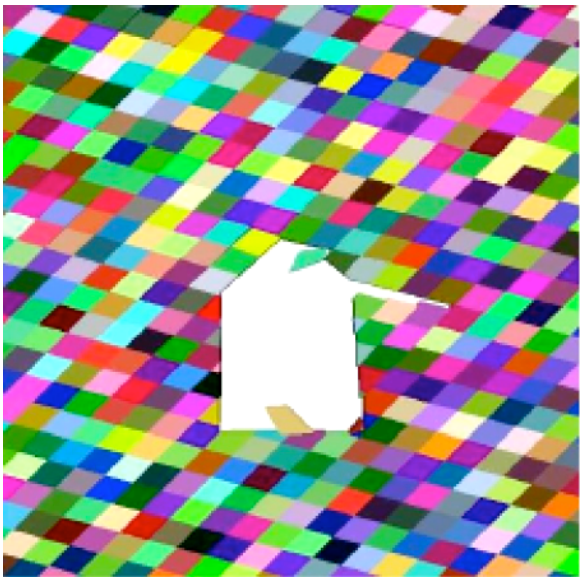

c) Joint set 2 dipping 15 degrees

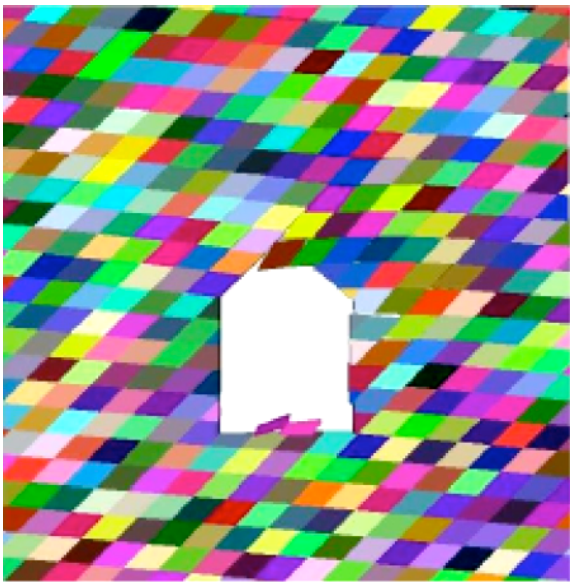

d) Joint set 2 dipping 5 degrees

Fig. 23. Stability of tunnels under gravity in geology 1, with changes in the dip of joint set 2

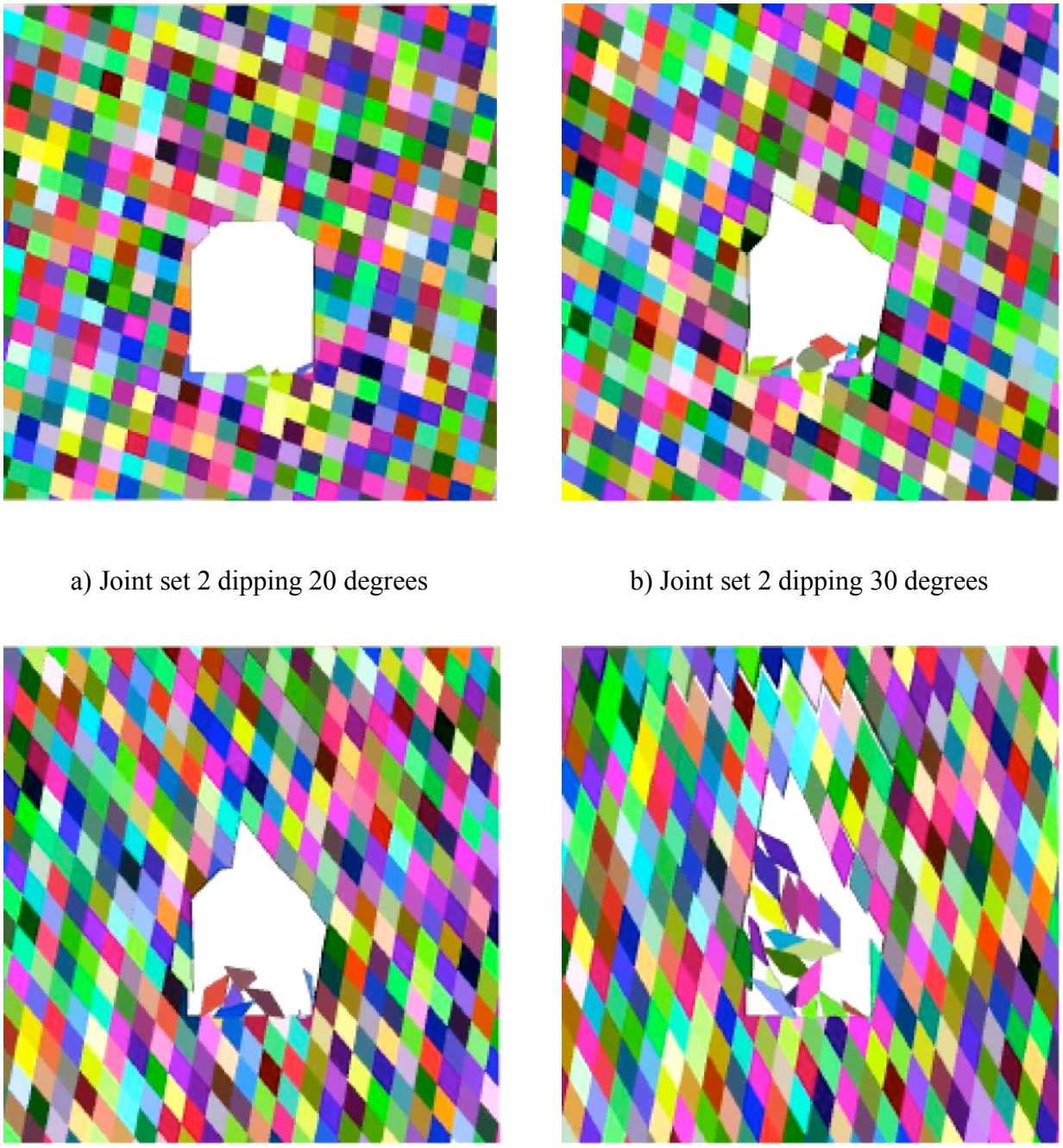

a) Joint set 2 dipping 20 degrees

b) Joint set 2 dipping 30 degrees

c) Joint set 2 dipping 50 degrees

d) Joint set 2 dipping 60 degrees

Fig. 24. Stability of tunnels under gravity in geology 2, with changes in the dip of joint set 2

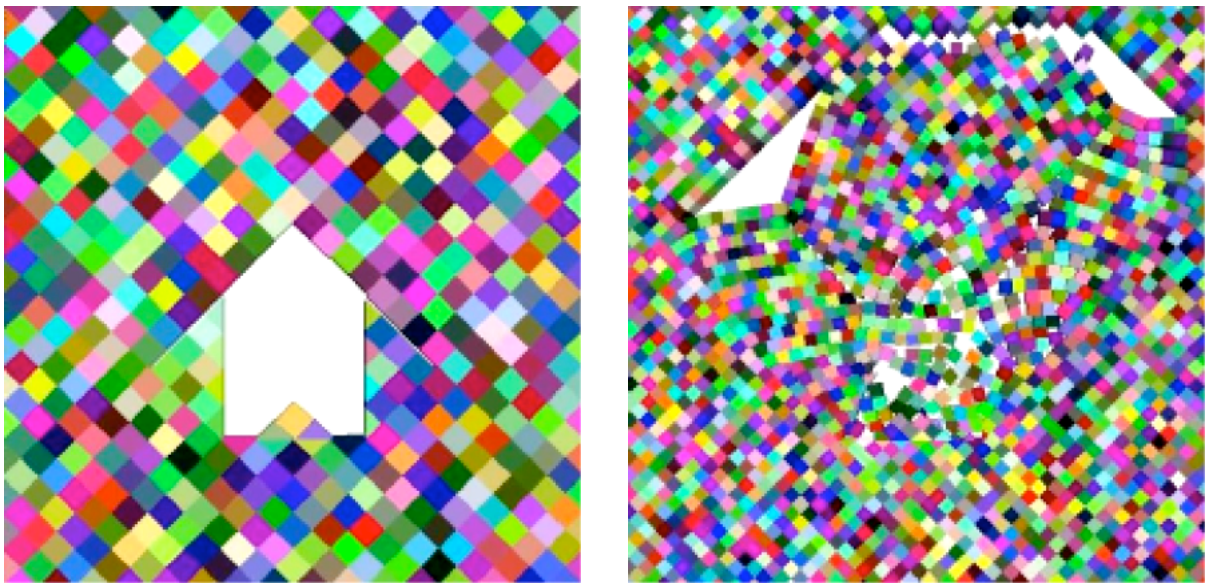

a) Spacing of joint sets 70cm b) Spacing of joint sets 35cm

Fig. 25. Influence of the spacing of joint sets on tunnel stability in geology 1 under gravity only

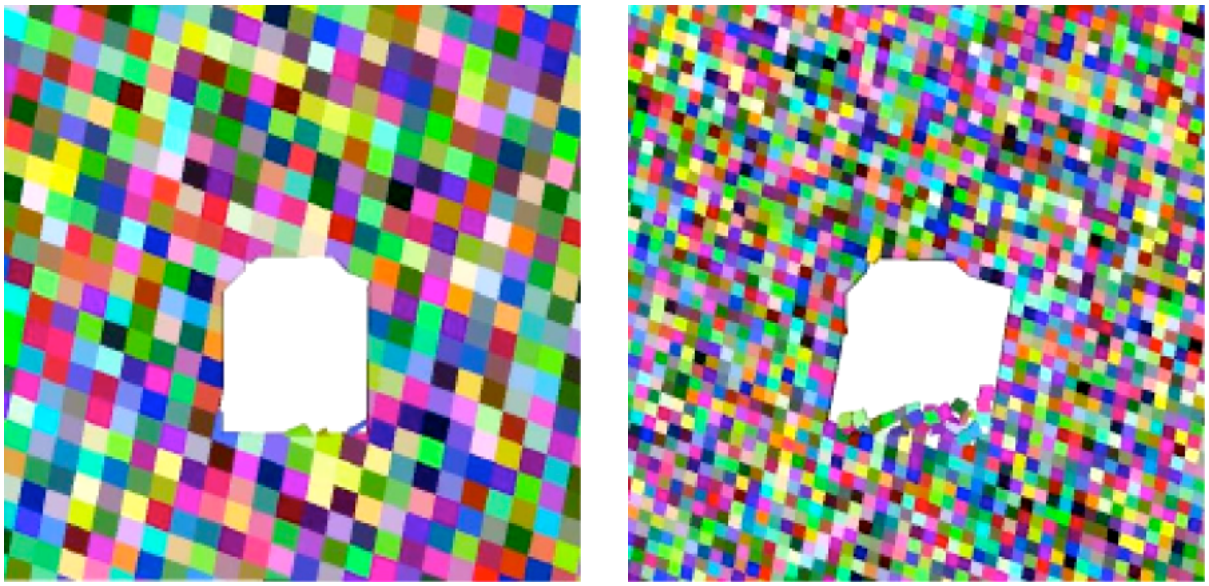

a) Spacing of joint sets 70cm b) Spacing of joint sets 35cm

Fig. 26. Influence of the spacing of joint sets on tunnel stability in geology 2 under gravity only

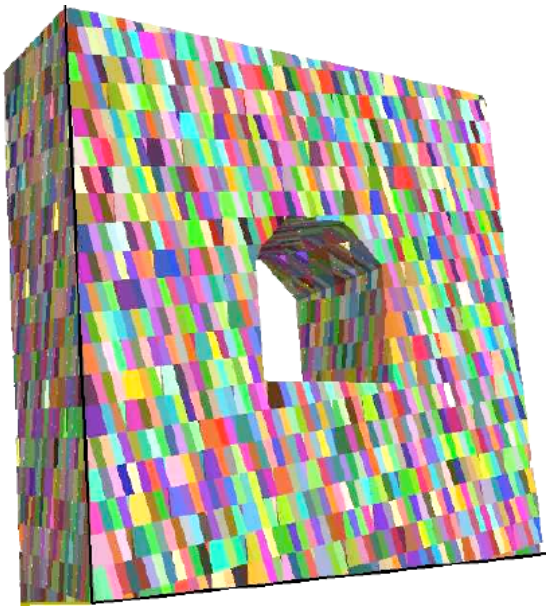

a) Geology 3 – 10742 rock blocks

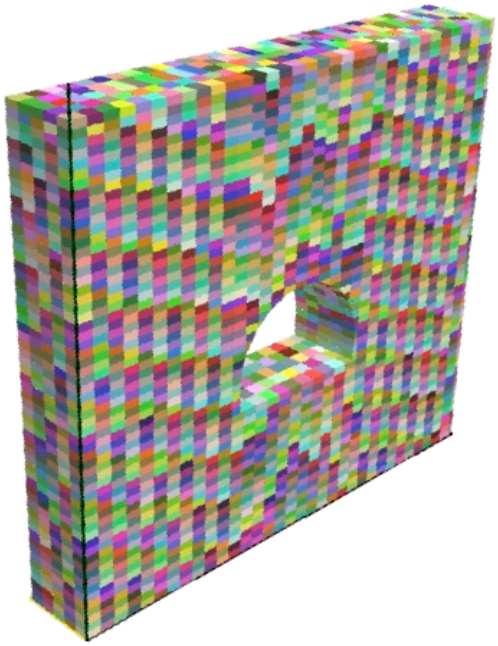

b) Geology 4 – 9695 rock blocks

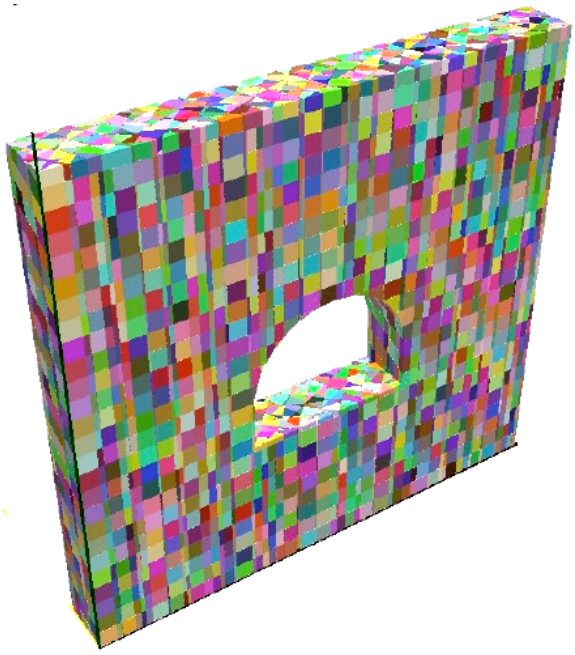

c) Geology 5 – 11592 rock blocks

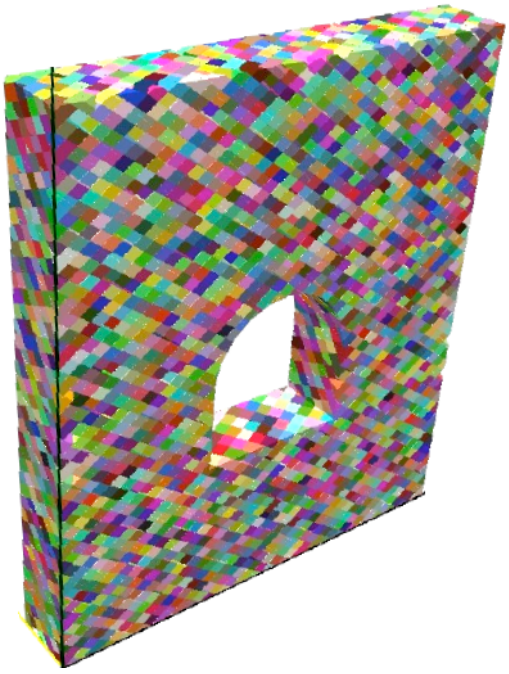

d) Geology 6 - 12432 rock blocks

Fig. 27. Rock islands with tunnel used in LDEC simulations for examination of the effect of joint set continuity on tunnel resistance against ground shock

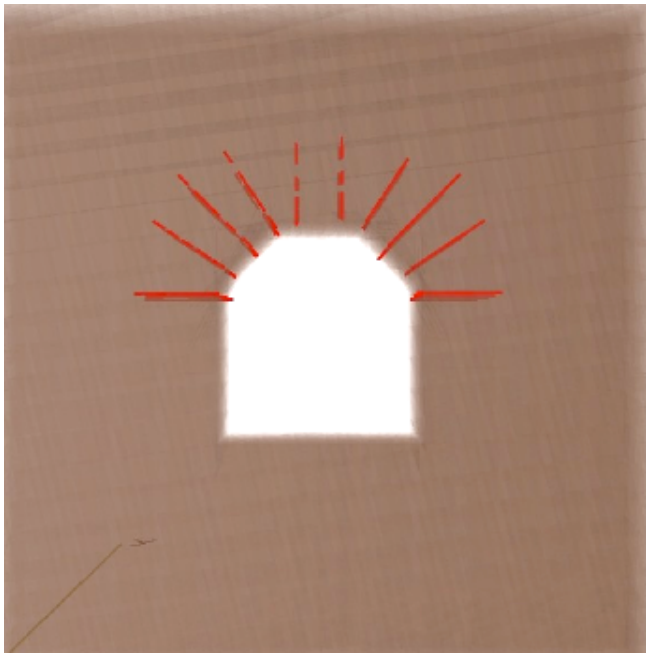

Fig. 28. Bolting pattern used for unlined tunnel in geology 3
(1.2-m long bolts on 1-m spacing)

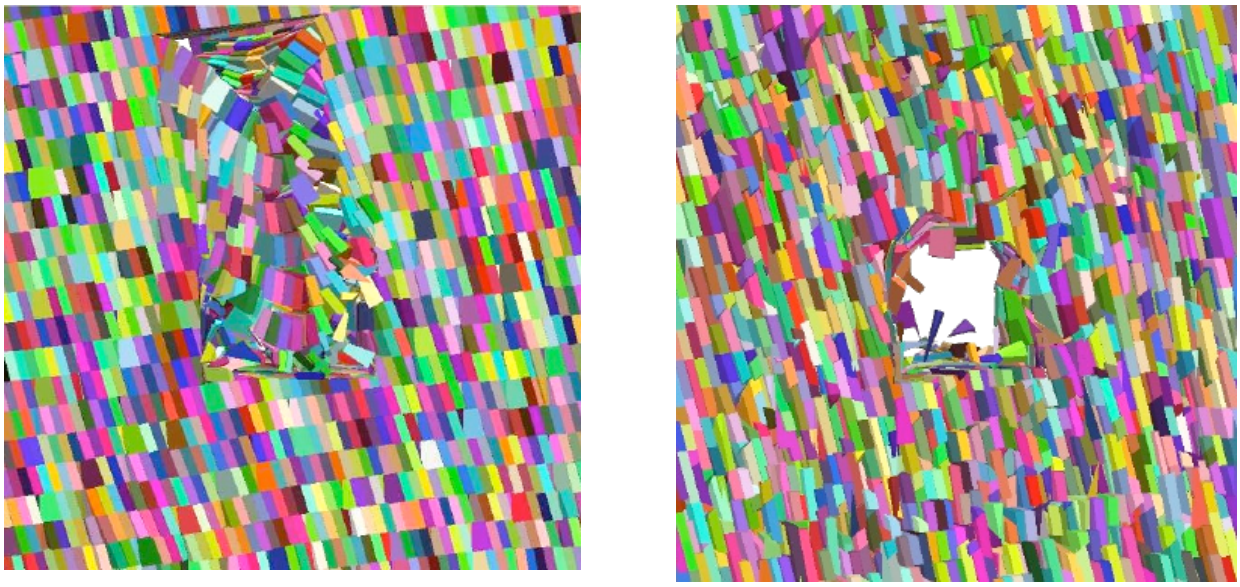

a) 100% persistent joints – 10726 blocks

b) 50% persistent joints – 8556 blocks

Fig. 29. Stability of an unlined tunnel in geology 3 for two values of joint persistence

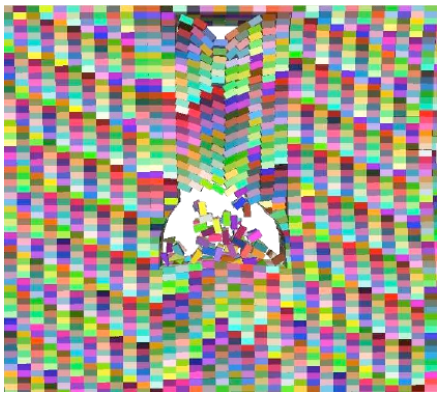

a) 100% joint persistence – 9695 blocks

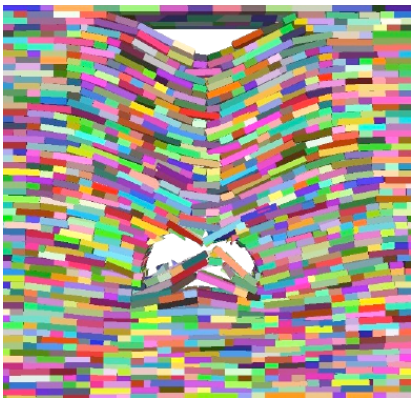

b) 50% joint persistence – 4030 blocks

Fig. 30. Stability of an unlined tunnel in geology 4 for two values of joint persistence

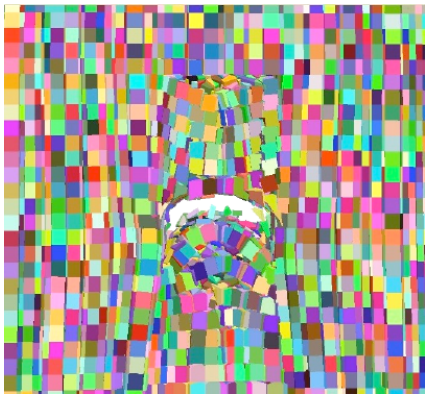

a) 100% joint persistence – 11588 blocks

b) 50% joint persistence – 4309 blocks

Fig. 31. Stability of an unlined tunnel in geology 5 for two values of joint persistence

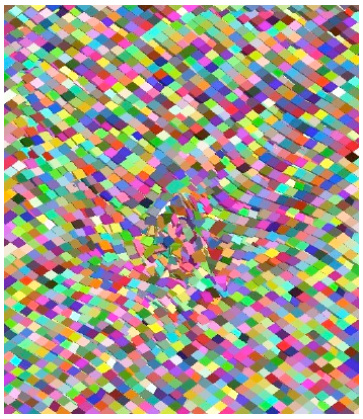

a) 100% joint persistence – 12430 blocks

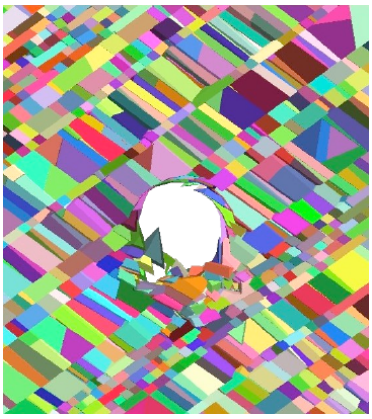

b) 50% joint persistence – 2170 blocks

Fig. 32. Stability of an unlined tunnel in geology 6 for two values of joint persistence

a) 100% joint persistence – 9930 blocks b) 50% joint persistence – 4167 blocks

Fig. 33. Stability of a lined tunnel in geology 4 for two values of joint persistence

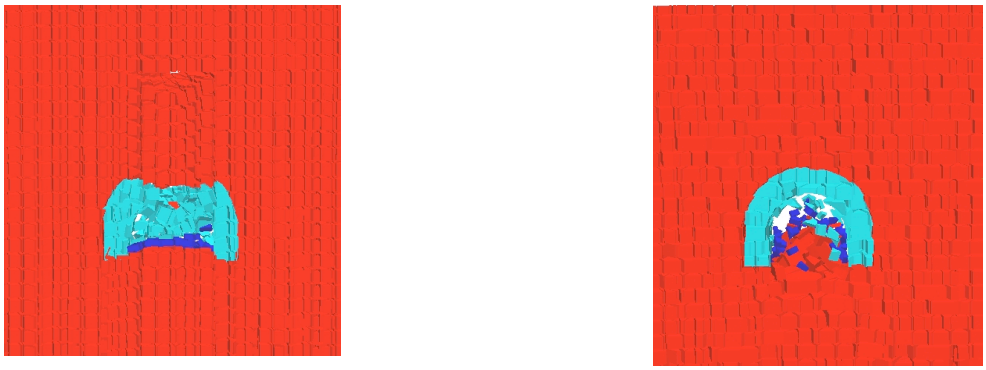

a) 100% joint persistence – 12145 blocks b) 50% joint persistence – 4448 blocks

Fig. 34. Stability of a lined tunnel in geology 5 for two values of joint persistence

a) 100% joint persistence – 13645 blocks b) 50% joint persistence – 2201 blocks

Fig. 35. Stability of a lined tunnel in geology 6 for two values of joint persistence

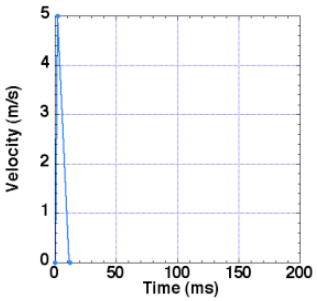

a) D= 3.125cm

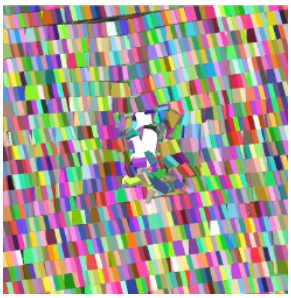

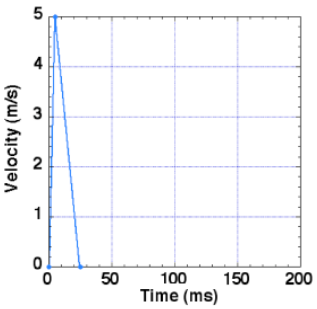

b) D = 6.25cm

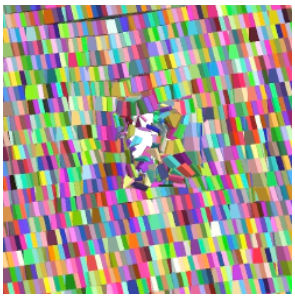

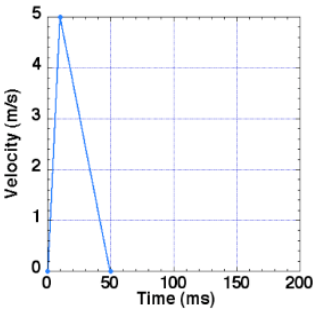

c) D = 12.5cm

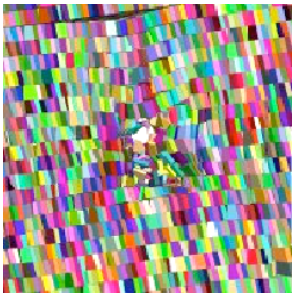

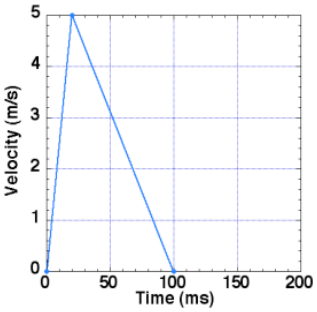

d) D = 25cm

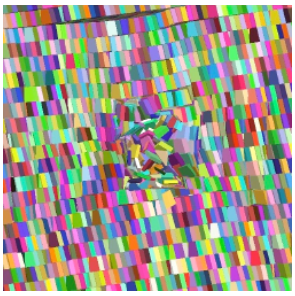

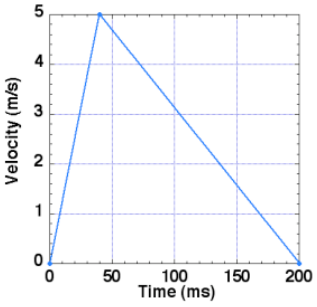

e) D = 50cm

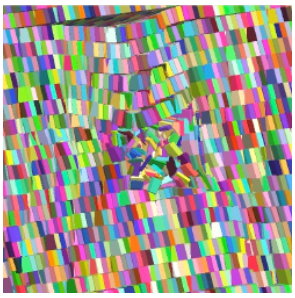

Fig. 36 Effect of total displacement (D) on tunnel stability from a 5m/s peak velocity pulse

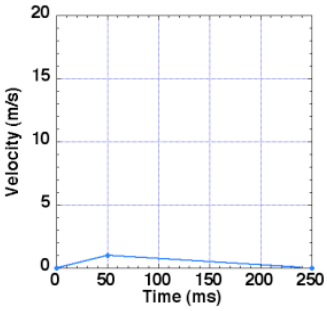

a) V = 1m/s

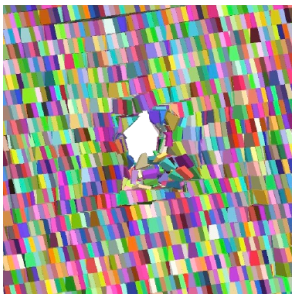

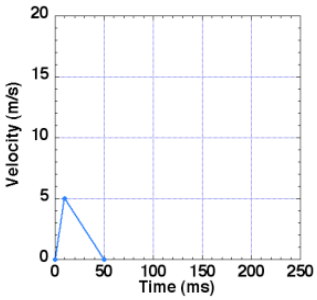

b) V = 5m/s

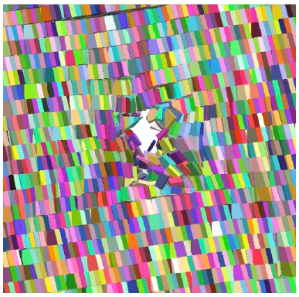

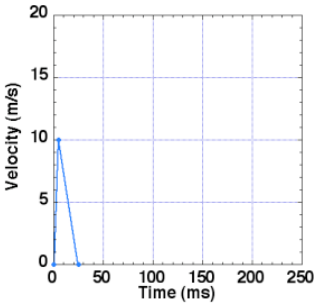

c) V = 10m/s

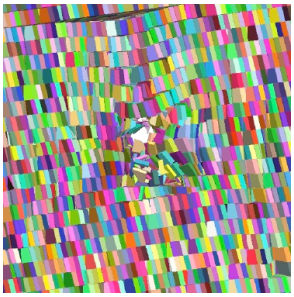

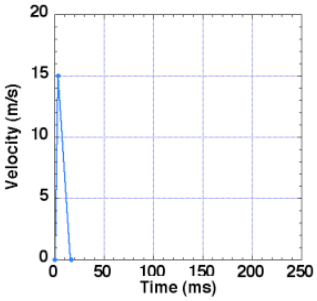

d) V = 15m/s

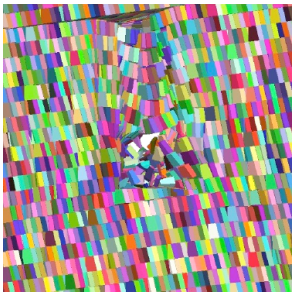

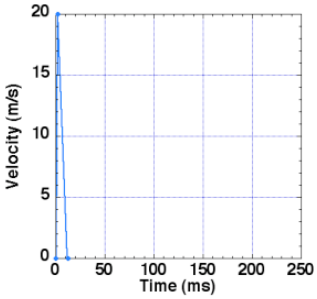

e) V = 20m/s

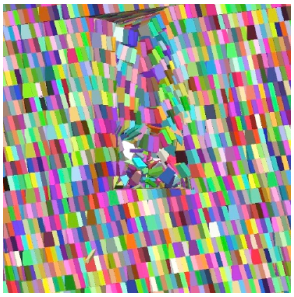

Fig. 37. Effect of peak velocity on tunnel stability from a 12.5cm peak displacement pulse

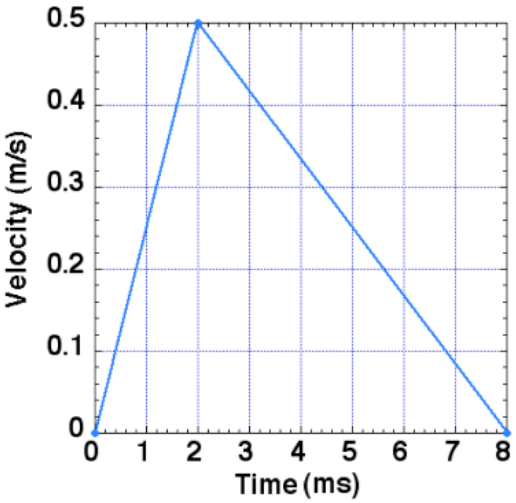

a) D = 0.2cm

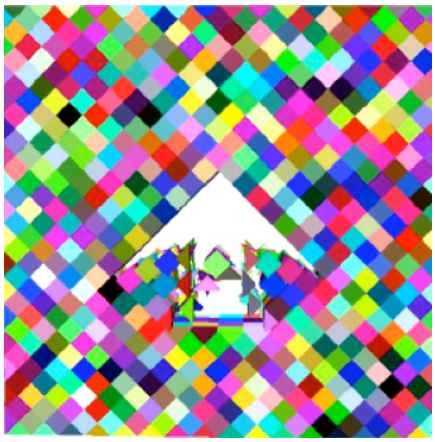

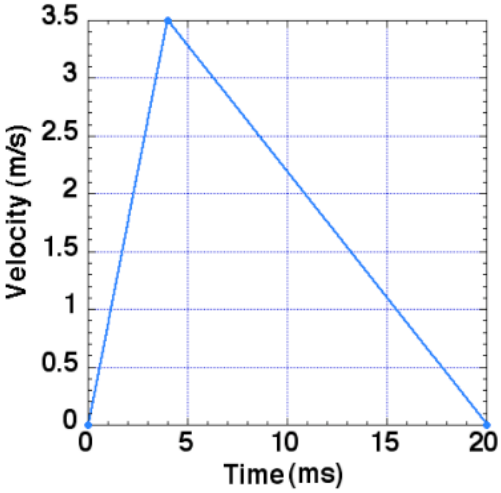

b) D = 3.5cm

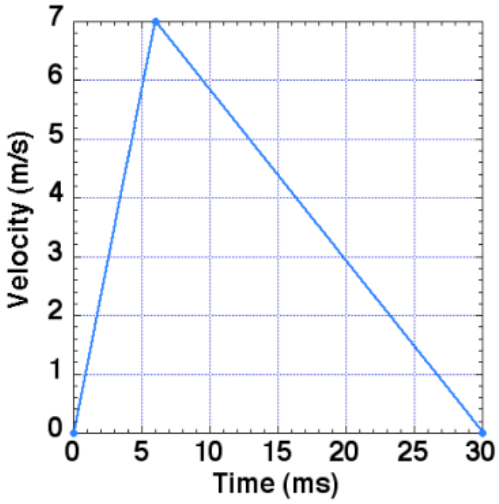

c) D = 10.5cm

Fig.38. Effects of successive pulses on an unlined tunnel. Note that after the first ground shock the tunnel assumed a more robust shape that was not affected by even stronger loadings.

Fig. 39. Stable (?) roof arch created by a strong ground shock in volcanic tuff, Nevada, USA

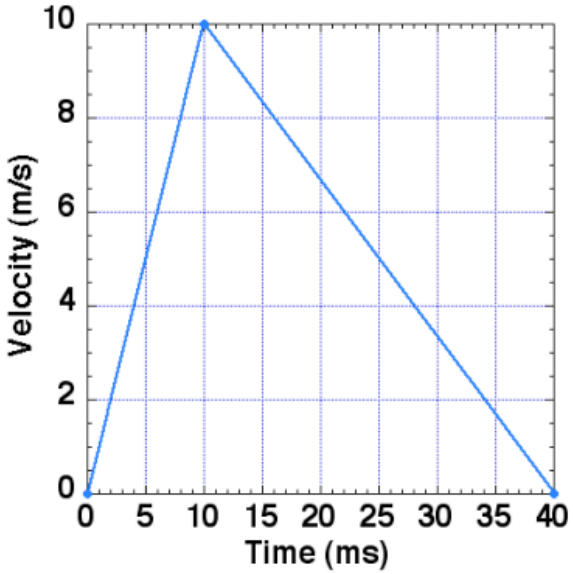

a) Loading pulse applied twice in a row to the top of the rock island of Fig. 27b. The total displacement of each pulse is 20cm.

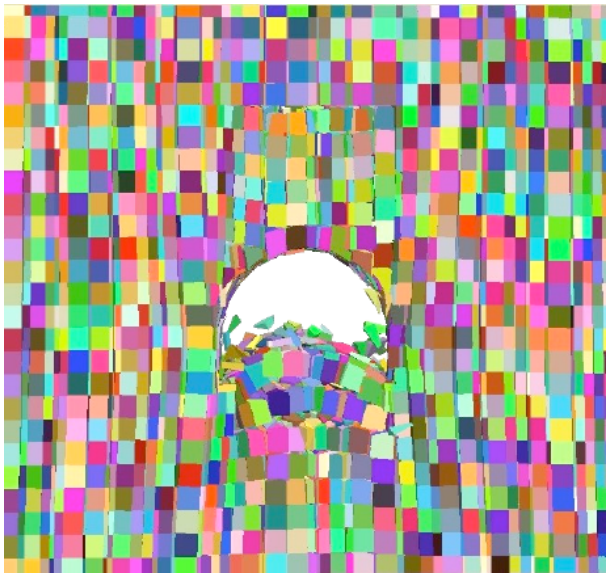

b) Result after the first pulse

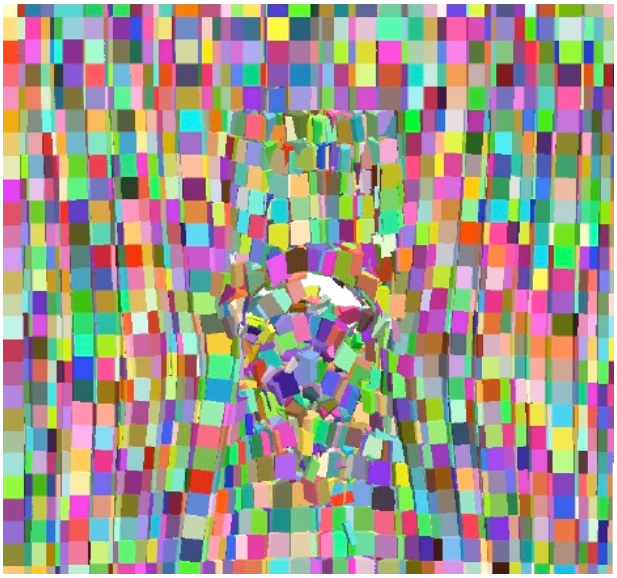

c) Result after the second pulse

Fig. 40. An unlined tunnel experiencing cumulative damage from repeated loadings. The first ground shock creates moderate damage and the second shock destroys the tunnel.

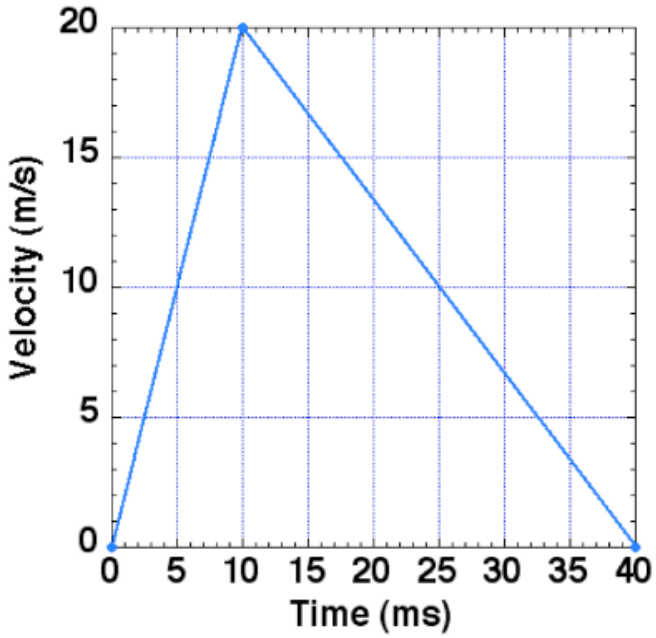

a) Velocity pulse applied twice in a row vertically to the top of the rock island of Fig. 27c, with a lined tunnel. The total displacement of each pulse is 40cm.

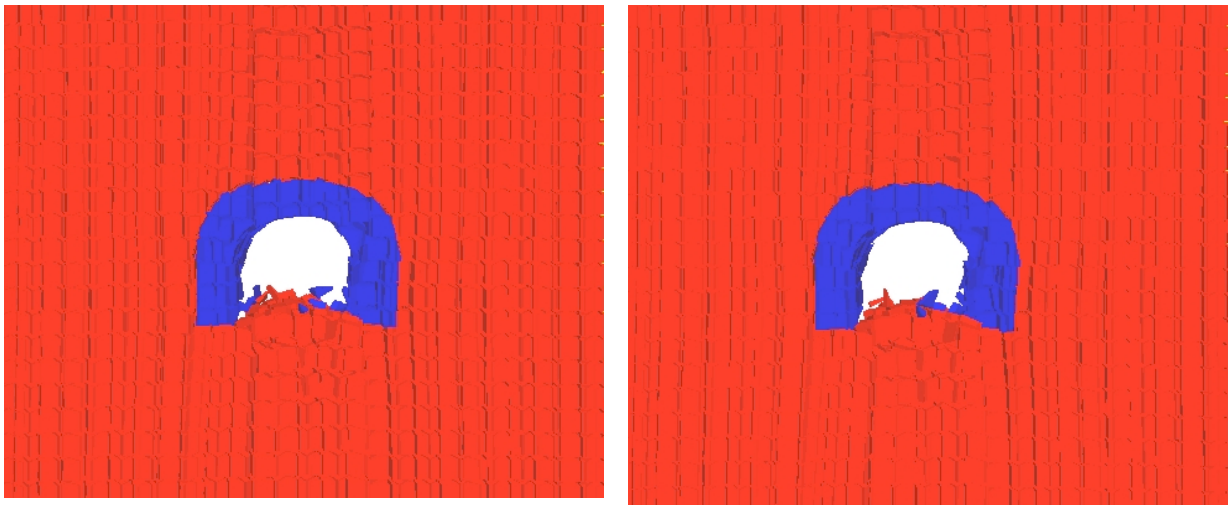

b) Result after the first pulse

c) Result after the second pulse

Fig. 41. Effects of repeated loading on a reinforced concrete lined tunnel. After the liner withstood the first ground shock with little damage, the second ground shock had no further effect.

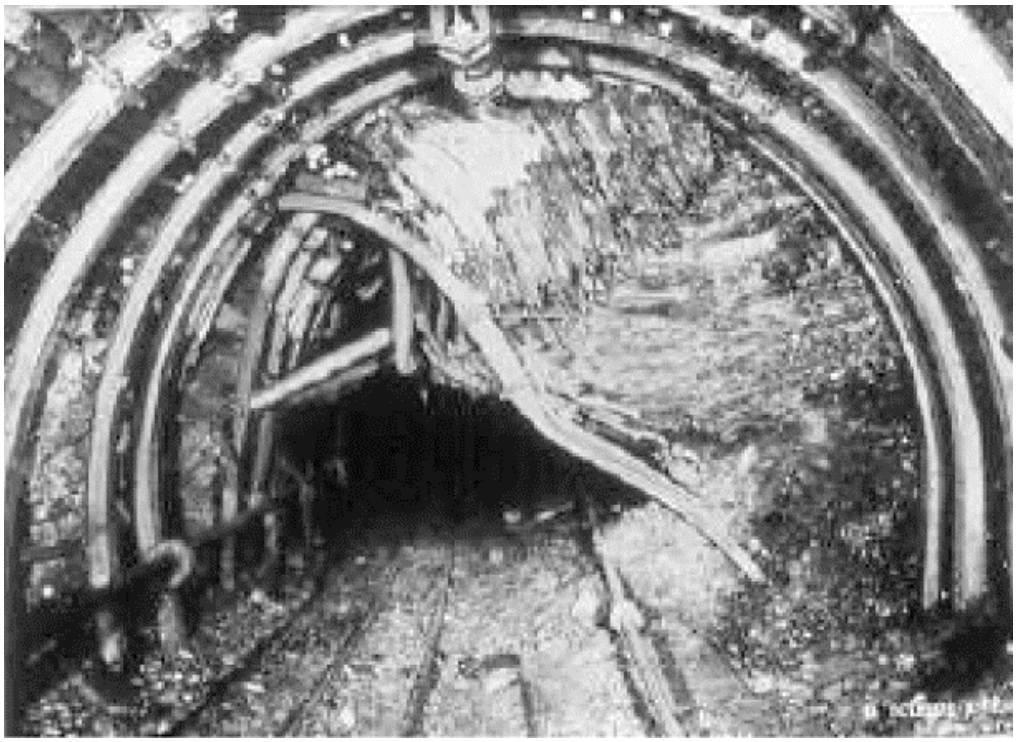

a) Buckling of thin coal measure rock layers due to bump in a Belgian coal mine (courtesy of Dr. Stassen, 1985)

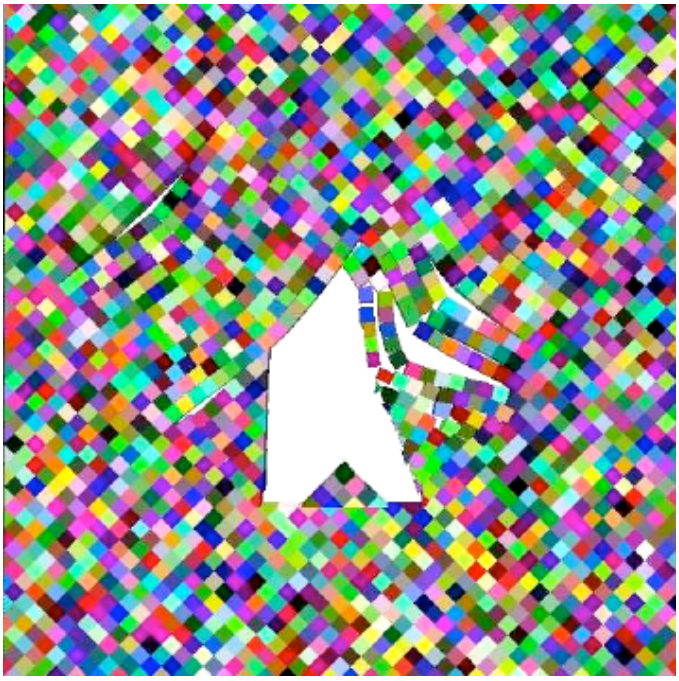

b) LDEC calculation showing buckling of thin layers

Fig. 42. LDEC capturing a phenomenology seen in thinly bedded rock formations

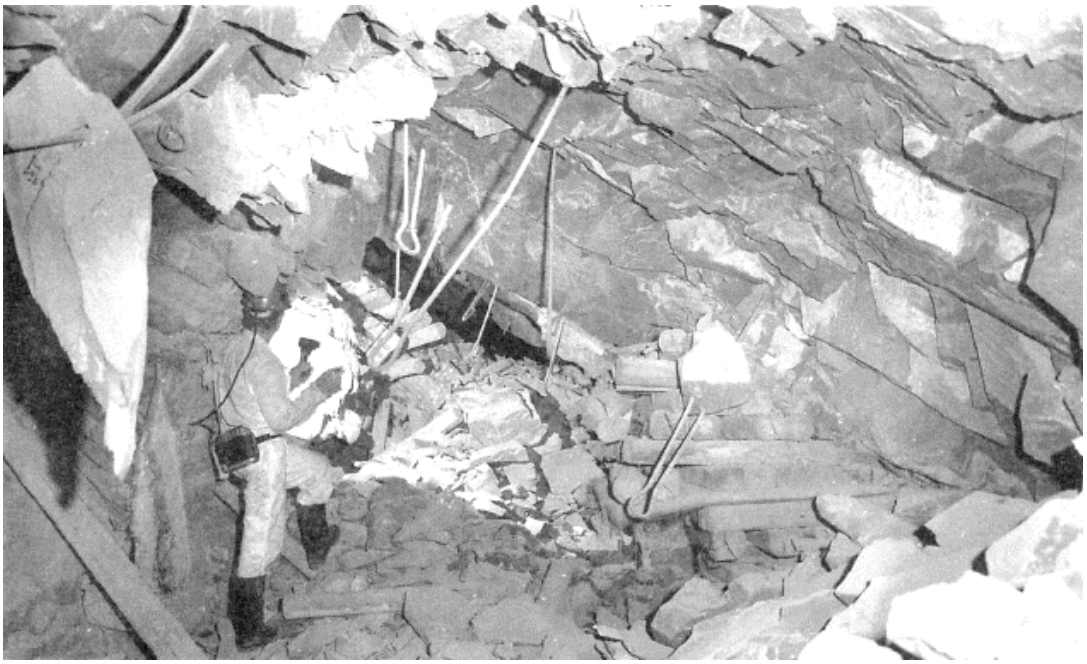

a) Fairly symmetrical roof collapse and floor rubble due to a rock burst in a South Africa gold mine (courtesy of Dr. Ortlepp, 2003)

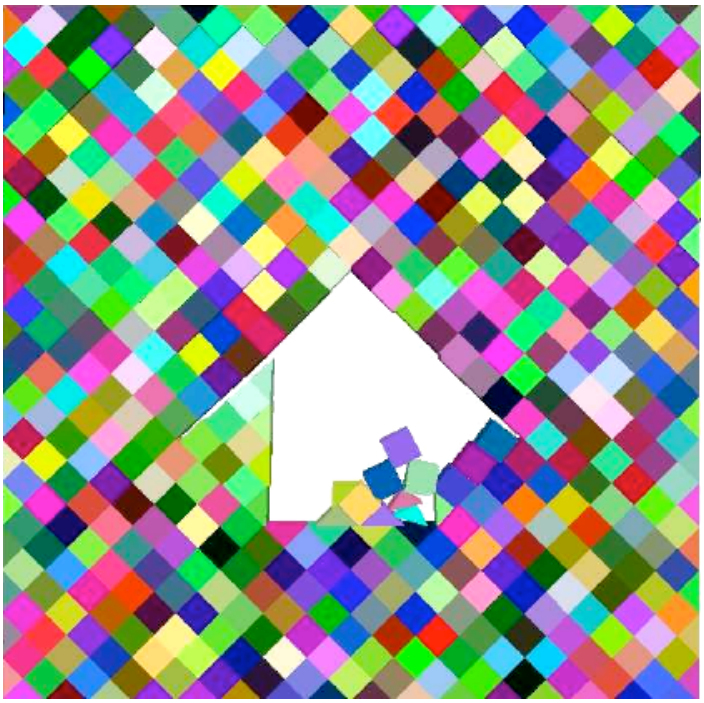

b) LDEC simulation showing a fairly symmetrical roof collapse due to symmetrical jointing

Fig 43. Rock mass failure phenomenology captured by LDEC (cont.)

a) Unsymmetrical roof collapse and floor rubble due to a rock burst in a South Africa gold mine (courtesy of Dr. Ortlepp, 2003)

b) LDEC showing a non-symmetric roof failure controlled by the jointing

Fig. 44. Rock mass failure phenomenology captured by LDEC (cont.)

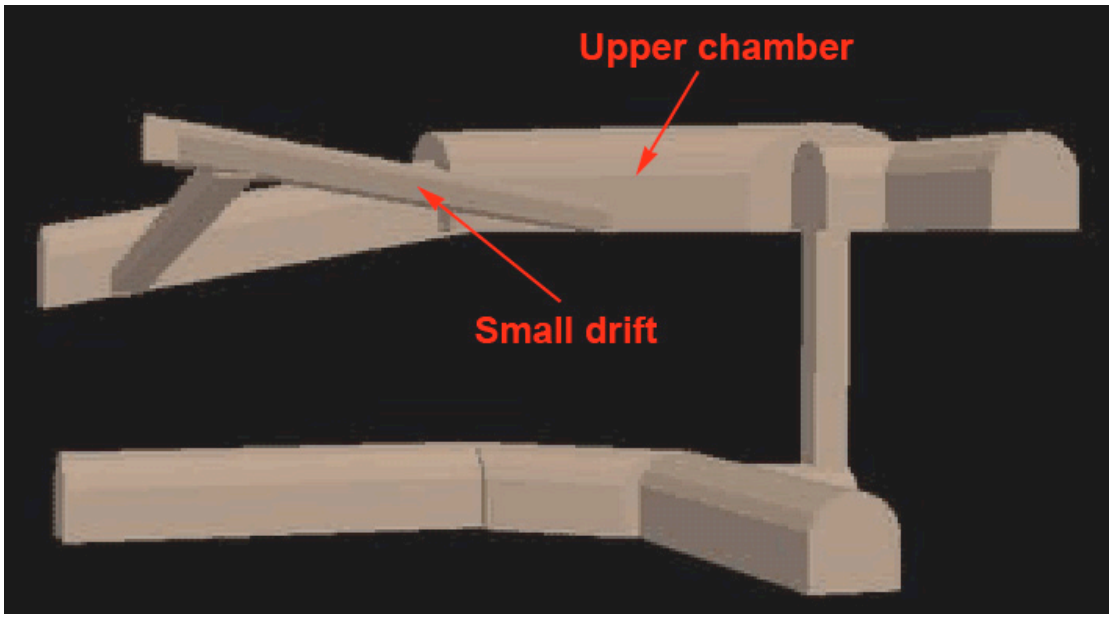

Fig.45. Underground facility subjected to ground shock, analyzed with a massively parallel LDEC simulation.

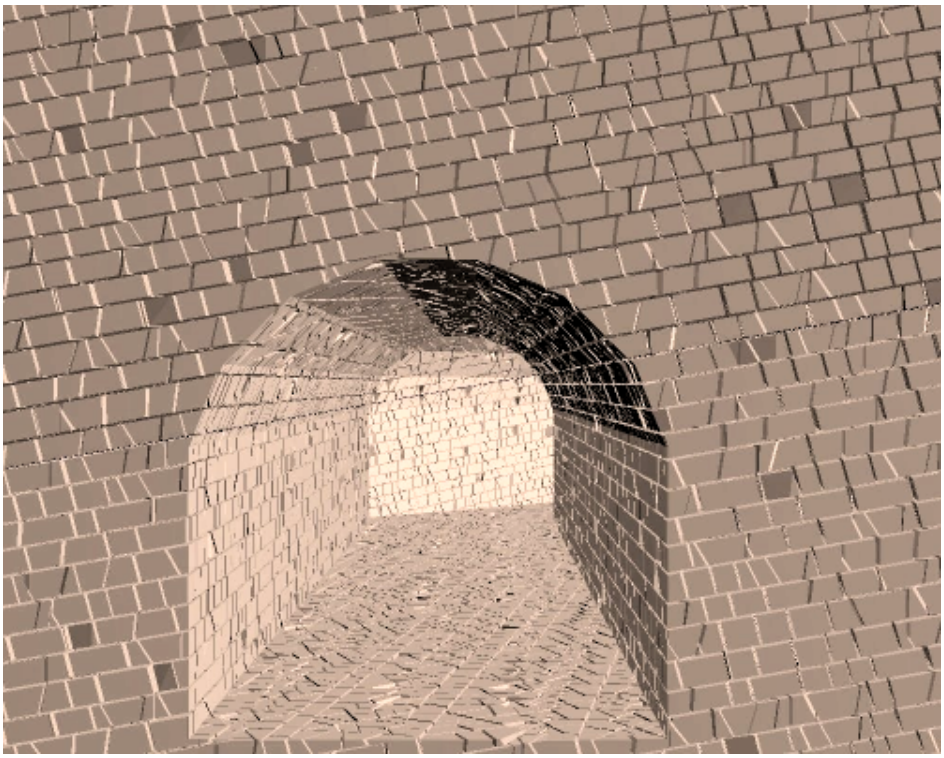

Fig.46. Geologic structure resulting from continuous sub-horizontal joints and non-persistent steeply dipping joints

Fig. 47. View along the length of the upper chamber

Fig. 48. View of the small drift from the inside of the upper chamber. The drift appears to be destroyed.

Fig. 49. View from inside the small drift, looking towards the upper chamber. That observation location reveals that part of the drift is undamaged.

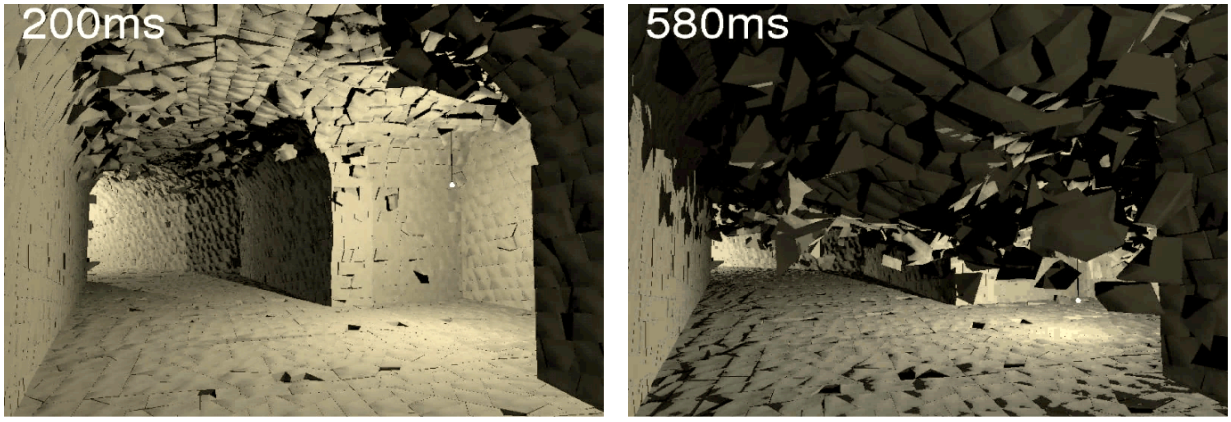

Fig. 50 Response to the ground shock at the intersection of the shaft and L3. Note that the L2 section is stable.

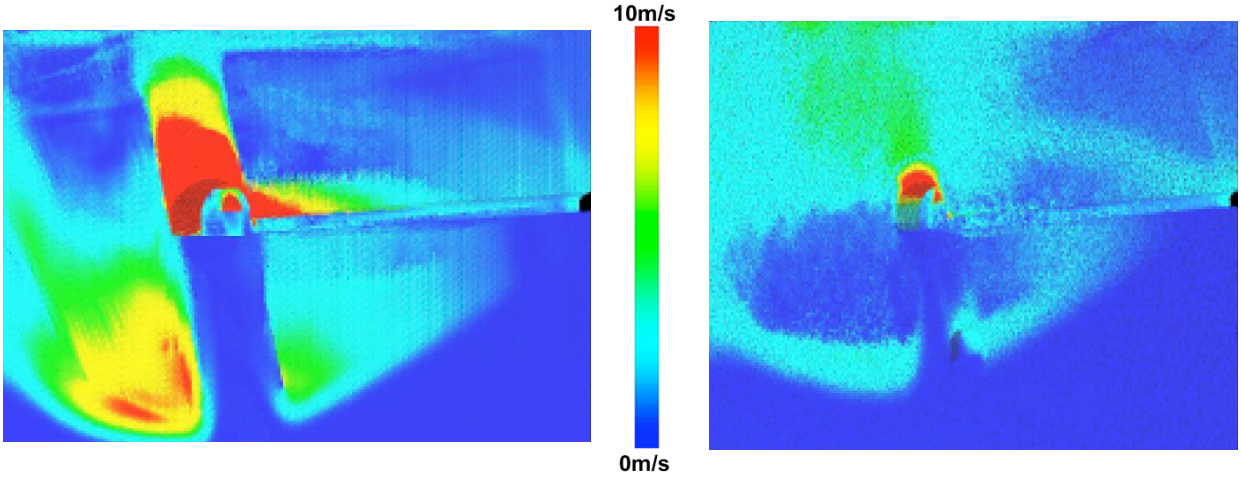

a) Continuous joints

b) Non-persistent joints

Fig. 51. Comparison of the velocity field at 30ms in a section across the upper chamber and the small upper drift, under two assumptions of joint continuity.